Available online at www.sciencedirect.com
SCIENCE DIRECT
Developmental Biology 288 (2005) 160 – 178
DEVELOPMENTAL BIOLOGY
www.elsevier.com/locate/ydbio

The insect homologue of the amyloid precursor protein interacts with the heterotrimeric G protein Goα in an identified population of migratory neurons

T.L. Swanson, L.M. Knittel, T.M. Coate, S.M. Farley, M.A. Snyder, P.F. Copenhaver *

Department of Cell & Developmental Biology, L-215, Oregon Health & Science University, 3181 SW Sam Jackson Park Road, Portland, OR 97239, USA

Received for publication 16 April 2005, revised 1 September 2005, accepted 6 September 2005
Available online 17 October 2005

Abstract

The amyloid precursor protein (APP) is the source of Aβ fragments implicated in the formation of senile plaques in Alzheimer's disease (AD). APP-related proteins are also expressed at high levels in the embryonic nervous system and may serve a variety of developmental functions, including the regulation of neuronal migration. To investigate this issue, we have cloned an orthologue of APP (msAPPL) from the moth, *Manduca sexta*, a preparation that permits in vivo manipulations of an identified set of migratory neurons (EP cells) within the developing enteric nervous system. Previously, we found that EP cell migration is regulated by the heterotrimeric G protein Goα: when activated by unknown receptors, Goα induces the onset of Ca^{2+} spiking in these neurons, which in turn down-regulates neuronal motility. We have now shown that msAPPL is first expressed by the EP cells shortly before the onset of migration and that this protein undergoes a sequence of trafficking, processing, and glycosylation events that correspond to discrete phases of neuronal migration and differentiation. We also show that msAPPL interacts with Goα in the EP cells, suggesting that msAPPL may serve as a novel G-protein-coupled receptor capable of modulating specific aspects of migration via Goα-dependent signal transduction.

Keywords: Neuronal migration; Amyloid; APP; G protein; *Manduca sexta*

Introduction

A hallmark feature of Alzheimer's disease (AD) is the accumulation of amyloid plaques in the brain (Glenner and Wong, 1984; Masters et al., 1985), which are formed predominantly by short β-amyloid fragments (Aβ) that are derived by proteolytic cleavage of the amyloid precursor protein (APP; Kang et al., 1987; Suh and Checler, 2002). APP is a member of a family of transmembrane glycoproteins with structural similarity to cell surface receptors: they possess large extracellular domains with several potential protein interaction motifs, plus short cytoplasmic domains containing motifs that can interact with a variety of adapter and intracellular signaling molecules (Annaert and De Strooper, 2002; Turner et al., 2003). At least 10 distinct isoforms of APP may be generated via alternative mRNA splicing from a single gene (Sandbrink et al., 1994a,b), but the predominant isoform expressed in the nervous system is APP_{695} (Kitaguchi et al., 1988). Proteolytic cleavage of APP by a combination of juxtamembrane and intramembrane secretases results in the release of the Aβ fragment, which can then aggregate into amyloid plaques (Selkoe, 1998, 2000). Both the soluble Aβ monomer (Tong et al., 2004; Yankner, 1996) and its aggregates (Klein, 2002; Selkoe, 2001; Stern et al., 2004) are capable of inducing a variety of neurotoxic effects, providing support for the "amyloid hypothesis" that this cleavage product of APP mediates the neurodegenerative aspects of Alzheimer's disease (Hardy and Allsop, 1991; Hardy and Selkoe, 2002; Greeve et al., 2004).

However, more recent studies on the biological actions of APP have impelled a modified view of this hypothesis. APP is expressed at high levels in the developing nervous system and is localized to regions of neuronal motility and synapse formation (Akaaboune et al., 2000; Loffler and Huber, 1992; Masliah et al., 1992). APP has been detected within growth cones and developing synapses in the mammalian brain (Akaaboune et al., 2000; Clarris et al., 1995; Kirazov et al., 2001; Lahiri et al., 2002) and is upregulated in regenerating

* Corresponding author. Fax: +1 503 494 4253.
E-mail address: copenhav@ohsu.edu (P.F. Copenhaver).

0012-1606/$ - see front matter © 2005 Elsevier Inc. All rights reserved.
doi:10.1016/j.ydbio.2005.09.029

olfactory neurons (Struble et al., 1998). In cell culture, APP can also promote neurite outgrowth (Beher et al., 1996; Qiu et al., 1995) and cell–substratum adhesion (Chen and Yankner, 1991; Kibbey et al., 1993). These observations have led to the proposal that APP is part of a large protein complex normally involved in the regulation of such processes as neuronal migration, axonal outgrowth, and synaptic differentiation (Sabo et al., 2001; Turner et al., 2003), albeit via poorly defined mechanisms.

More provocative is the co-localization of APP with a number of molecules in focal complexes at the leading edges of migratory cells. These include β-integrins (Yamazaki et al., 1997), which may provide a functional link between APP and the actin cytoskeleton, and the adapter proteins Fe65, mDAB1, and members of the X11/Mint family, each of which can bind to the cytoplasmic domain of APP (Sabo et al., 2001). APP also directly interacts with the heterotrimeric G protein Goα (Nishimoto et al., 1993; Giambarella et al., 1997; Okamoto et al., 1996), a signal transduction molecule that comprises up to 1% of all membrane-associated protein in the developing nervous system (Edmond et al., 1990) but whose developmental functions remain poorly understood. Indeed, APP has been postulated to act as a novel class of G-protein-coupled receptor (Brouillet et al., 1999; Giambarella et al., 1997), although the importance of this interaction with respect to the control of neuronal growth and survival is still controversial (Turner et al., 2003). Both APP and its proteolytic products are capable of exerting a variety of actions on cell growth, signal transduction, and neural plasticity (Kamenetz et al., 2003; Li et al., 1997; Mucke et al., 1994; Walsh et al., 2002), leading to the proposal that APP may serve as a "molecular hub" at the center of many converging regulatory pathways (Turner et al., 2003). Thus, besides the generation of excessive Aβ, aberrant processing of APP might disrupt one or more of its normal functions in the brain, which might in turn contribute to the abnormalities detected in AD. Yet despite a plethora of studies on APP and its fragments in a variety of assays, the developmental and physiological roles of APP have remained unclear.

Analysis of the intrinsic functions of APP in vertebrates has been complicated by the identification of two closely related proteins (APLP1 and APLP2) which share partially overlapping functions with APP (Heber et al., 2000; von Koch et al., 1997). In contrast, only one APP-related gene is expressed in *Drosophila* (*appl*; Rosen et al., 1989) and *Caenorhabditis* (*apl-1*; Daigle and Li, 1993), which has facilitated investigations into their normal functions in vivo. The proteins encoded by these genes share a number of structural similarities with the vertebrate APP family (Coulson et al., 2000), including the conserved intracellular domain required for Goα interactions (Nishimoto et al., 1993; Torroja et al., 1999b). Moreover, transgenic studies in *Drosophila* have shown that human APP_{695} can rescue at least some of the deficits caused by the deletion of APPL (Luo et al., 1992), demonstrating that these proteins are functionally as well as structurally conserved. In *Drosophila*, APPL has been implicated in variety of developmental functions, including the acquisition of phototactic behavior (Luo et al., 1992), axonal transport (Gunawardena and Goldstein, 2001; Torroja et al., 1999a), and postembryonic differentiation of neuromuscular synapses (Ashley et al., 2005; Torroja et al., 1999b). In particular, Torroja et al. found that selective mutations of the putative Goα-binding domain of APPL caused specific alterations in the growth of presynaptic boutons at the neuromuscular junctions (Torroja et al., 1999b), lending support to the model that APP-related proteins may functionally interact with Goα in developing neurons.

Surprisingly, genetic deletions of APPL in *Drosophila* produced only subtle effects on the developing nervous system (Li et al., 2004; Luo et al., 1992; Zambrano et al., 2002), possibly due to compensatory interactions by other functionally related proteins that may have masked the normal contribution of APPL to neural development. As an alternative means of addressing this issue, we have examined the developmental role of APPL during the formation of the enteric nervous system (ENS) in the moth *Manduca sexta*. The ENS in this species contains a distributed population of neurons (the EP cells) that occupy a branching nerve plexus (the enteric plexus) spanning the foregut–midgut boundary (Copenhaver and Taghert, 1988, 1989b; see Fig. 1). In previous work, we showed that the EP cells achieve their mature distributions in the enteric plexus via directed migration along identified sets of visceral muscles that form on the surface of the gut. After delaminating from the foregut epithelium, small groups of EP cells align with one of eight longitudinal muscle bands on the midgut or with specific radial muscles on the foregut (Fig. 1, 55% of development). Subsequently, the neurons migrate rapidly along these pathways (between 55 and 65% of development) before completing their differentiation (Copenhaver and Taghert, 1989b; Copenhaver et al., 1996). Of note is that throughout their development, the EP cells grow on the most superficial layer of the developing gut musculature; thus, both the neurons and their pathways remain accessible to direct observations and acute manipulations in embryonic culture (Horgan et al., 1995; Wright and Copenhaver, 2000).

The guidance of EP cell motility is also precisely regulated: although they continually extend short filopodial processes onto the adjacent interband musculature (Fig. 1, 55–60% of development), both the migrating neurons and their growing axons remain closely apposed to their muscle band pathways, only branching laterally to innervate the interband regions towards the end of their differentiation (Fig. 1, 100% of development). In part, the precise guidance of the EP cells is mediated by fasciclin II (mFas II), a homophilic adhesion receptor that is expressed by both the neurons and transiently the muscle bands during the migratory period (Wright and Copenhaver, 2000, 2001). However, strong repulsive interactions have also been found to prevent EP cell migration onto the interband regions (Copenhaver et al., 1996), a process that may be mediated by the G protein Goα. All of the neurons commence the expression of Goα just prior to the onset of migration, and selective activation of Goα within individual EP cells inhibits their motility in a Ca^{2+}-dependent manner (Horgan et al., 1994, 1995). However, the identity of candidate Goα-coupled receptors capable of inducing this response in the EP cells has remained unknown.

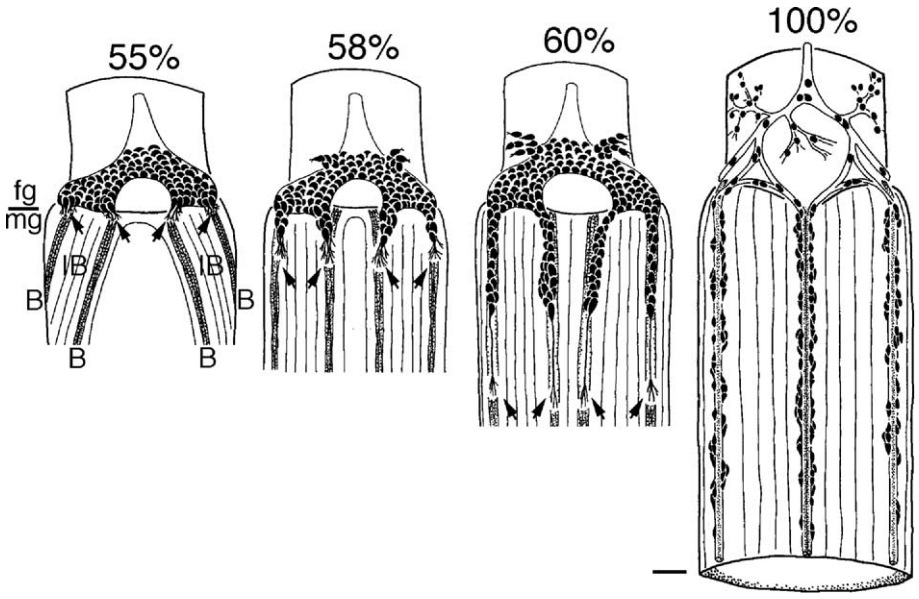

Fig. 1. Formation of the ENS in *Manduca* involves the stereotyped migration of the EP cells into the enteric plexus. Between 30 and 40% of development (not shown), the EP cells delaminate from a neurogenic placode to form a coherent packet of pre-migratory neurons on the dorsal foregut surface at the foregut–midgut boundary (Copenhaver and Taghert, 1990). Then, between 40 and 55% of development, the packet of EP cells (black cells) spreads bilaterally around the foregut–midgut boundary, and subsets of the neurons (arrows, 55%) gradually align with one of eight longitudinal muscle bands (B) that coalesce from the longitudinal muscle cells of the midgut (only the dorsal four muscle bands are shown). As midgut closure is completed (between 55 and 60% of development), the EP cells commence a rapid phase of migration onto the longitudinal muscle bands of the midgut and onto specific radial muscles on the foregut (radial muscles are not shown). During this period of active migration, each of the EP cells extends filopodial processes in advance of their cell body onto both their muscle band pathways and onto the adjacent interband regions (IB). However, both the migration (from 55 to 65% development) and subsequent outgrowth of these neurons (from 65 to 75% development) are restricted to the muscle bands, while they avoid the interband regions. Although the EP cells tend to migrate in small groups, each neuron moves independently, traveling over both the underlying muscle band cells and adjacent neurons in an apparently stochastic manner. By the completion of embryogenesis (100% of development), this migratory sequence has resulted in eight dispersed columns of neurons that are distributed along the anterior segments of each muscle band. Only after their migration and outgrowth are complete do the EP cells branch laterally onto the interband regions, providing a diffuse innervation of the lateral musculature (Copenhaver and Taghert, 1989a). Although the timing of migration and the pathways followed by the EP cells are highly stereotyped, their final positions along a muscle band are not; rather, these neurons subsequently express one of several distinct neuronal phenotypes that are regulated in part by their final location (Copenhaver et al., 1996). Because the EP cells and their muscle band pathways occupy the most superficial layer of the gut, these neurons remain accessible to direct observation and experimental manipulations throughout embryogenesis. Percentages indicate percent of development (1% development = 1 h of real time at 25°C). B = midgut muscle band; IB = interband regions; fg/mg = foregut–midgut boundary. Scale = 30 μm.

In the present study, we have isolated and sequenced the gene encoding APPL in *Manduca* (designated msAPPL), and we have analyzed its developmental expression and processing in the EP cells with respect to their migration and differentiation. We have also investigated whether msAPPL and Goα interact within the EP cells during their migration. The results of these studies suggest a novel role for APP-related proteins in the control of neuronal motility within the developing nervous system.

Materials and methods

Developmentally synchronized embryos were collected from a colony of *M. sexta* and maintained at 25°C; at this temperature, embryogenesis is completed in 100 h (1% development = 1 h). Developmental staging, immunoblots, and whole-mount immunohistochemistry were performed as previously described (Horgan and Copenhaver, 1998; Wright et al., 1998). Antibodies were used at the following concentrations: anti-mFas II: 1:20,000 (Wright et al., 1999); anti-ELAV 1:500 (Robinow and White, 1991; gift from Dr. Kalpana White); anti-*Drosophila* APPL: 1:1000 (dAPPL; gift from Drs. Kalpana White and Vivian Budnik); and affinity-purified anti-Goα: 1:100 (Horgan et al., 1995). We also generated two antibodies against msAPPL: anti-msAPPL-cyt against the C-terminal (CZ)YENPTYKYFEVKE sequence (used at 1:5000); and anti-msAPPL-ect against the extracellular domain (CZ)EDDDYTDADD-SAWPRPES sequence (used at 1:1000). For whole-mount immunostaining, primary antibodies were detected using the HRP-based ABC protocol of Vector laboratories (Burlingame, CA) or using fluorochrome-conjugated secondary antibodies (Cy3-conjugates from Jackson Labs, West Grove, PA; and Alexa-488 and -568 conjugates from Molecular Probes, Eugene, OR). Whole-mount immunostained preparations were then photographed by conventional microscopy or imaged by confocal microscopy, either with an Olympus Fluoview 300 laser scanning confocal head mounted on an Olympus BX51 microscope or with a BioRad 1024 ES laser scanning confocal microscope.

Primary neuronal cultures were prepared after the methods of Hayashi et al. (Hayashi and Hildebrand, 1990; Hayashi and Levine, 1992). Briefly, desheathed ganglia were harvested from P0–P1 stage *Manduca* pupae, enzymatically dissociated with trituration, and plated onto glass coverslips coated with Concanavalin A plus Laminin (4–5 ganglia per dish). After 4 days in L-15-based culture medium (Gibco; Carlsbad, CA) plus 10% fetal bovine serum (FBS), the neurons were rinsed and grown for 2 additional days in reduced protein L-15 medium (L-15 plus 1 μg/ml 20-hydroxyecdysone, 100 U/ml penicillin, 100 U/ml streptomycin; from Sigma; St. Louis, MO). The medium from the cultures was then harvested and concentrated to a final volume of 30 μl (using a 30 kDa cut-off Centricon spin concentrator; Amicon; Beverly, CA), while the neurons were harvested in RIPA buffer (150 mM NaCl, 1% IGEPAL, 0.5% deoxychoic acid, 1% SDS, 50 mM Tris pH 8.0) for immunoblot analysis.

For immunoblots, soluble protein was extracted from pooled tissue samples collected from synchronous groups of embryos in lysis buffer or from primary neuronal cultures as described above. The protein samples were then separated by polyacrylamide gel electrophoresis (after our published methods; Wright and Copenhaver, 2000) and transferred to nitrocellulose. Replicate blots were incubated either with the primary antibodies listed above, with pre-immune

sera, or with aliquots of the anti-msAPPL antibodies that had been pre-adsorbed against the synthetic peptides used as their antigens (in a 10:1 molar ratio). Aliquots of each anti-msAPPL antibody were also cross pre-adsorbed with the peptide epitope used to generate the other antibody as an additional control for the specificity of our adsorption protocol. Bound antibodies were then detected either with alkaline-phosphatase-conjugated secondary antibodies (1:2500; KPL; Gaithersburg, MD), detected by a colorimetric reaction or with HRP-conjugated secondary antibodies (anti-chicken at 1:10K from Promega, Madison, WI; other HRP-conjugated secondary antibodies at 1:10 K from Jackson Immunoresearch, West Grove, PA), and detected by chemiluminescence using the Supersignal WestPico kit from Pierce (Rockford, IL) or the enhanced Visualizer kit from Upstate (Lake Placid, NY).

A partial clone of *Manduca* APPL (msAPPL) was obtained from embryonic cDNA, using degenerate PCR primers against evolutionarily conserved domains of APP-related proteins from other species (Daigle and Li, 1993; Rosen et al., 1989; Wasco et al., 1992, 1993). ^{32}P-labeled probes derived from this clone were then used to isolate clones from a cDNA library (gift of Dr. James Nardi) that contained the full-length coding sequence for msAPPL. Nucleotide sequencing was performed on an ABI 377 automated fluorescence sequencer and analyzed using the DNASTAR suite of programs. For Northern blots, ^{32}P-labeled probes were prepared from a cDNA clone containing the 1.6 kb open reading frame of msAPPL and used to label blots of poly A$^+$ mRNA that had been isolated from embryos with the MicroPoly(A)-Purist kit from Ambion. The mRNA was separated on a 1% agarose gel, transferred to a nylon membrane, hybridized with probe overnight at 80°C, and exposed to film after extensive washing. Whole-mount in situ hybridization histochemical staining of staged embryos was performed following published methods (Wright et al., 1999; Patel and Goodman, 1992), using digoxigenin-labeled probes generated against the 1.6 kb cDNA clone encoding msAPPL. Bound probe was detected in filleted embryos using an alkaline-phosphatase-conjugated anti-digoxigenin antibody (1:2000; Roche).

For co-immunoprecipitation of APPL and Goα, tissues were collected from developmentally synchronous groups of embryos or from desheathed pupal ganglia and frozen on dry ice. The samples were then homogenized in RIPA buffer for 20 min at room temperature, spun briefly, and the supernatant pre-cleared with Gammabind Plus Sepharose beads (25 μl in 250 μl; from Pharmacia). Replicate samples were then incubated either with 1–10 μl of each anti-msAPPL antibody, pre-immune sera, or with aliquots of the anti-msAPPL antibodies that had been pre-adsorbed against their synthetic peptides, as described above. Antibodies were added to the tissue homogenates for 3–4 h at room temperature followed by the addition of 25 μl washed beads (pre-adsorbed with 1% IgG-free bovine serum albumin) for 1 h at room temperature. Beads with bound antibody were then pelleted by centrifugation, washed three times in chilled RIPA buffer, and then resuspended in SDS sample buffer (Wright et al., 1999). After boiling for 5 min, the total volume of the resuspended pellets or 30 μl aliquots of the residual supernatants from each immunoprecipitation reaction were separated on 12% SDS polyacrylamide gels, transferred to nitrocellulose, and immunoblotted with anti-Goα antibodies. Labeled bands were visualized using HRP-conjugated secondary antibodies detected with the Visualizer kit (Upstate).

For removal of N-linked glycoproteins from msAPPL, staged groups of embryos (at 65% of development) were homogenized in RIPA buffer plus protease inhibitors at room temperature for 15 min. Alternatively, the tissue samples were homogenized in hot extraction buffer (10% glycerol; 1% mM SDS, 50 mM Tris pH 6.7) plus inhibitors for 5 min at 100°C. The samples were cleared by brief (5 min) microcentrifugation, and the soluble fractions incubated with the deglycosylating enzyme PNGase F (Peptide: N-Glycosidase F; 500 U/μl; New England Biolabs; Beverly, MA) following the manufacturer's instructions for 16–24 h at 37°C. Control samples were treated in an identical manner but without the addition of PNGase. Replicate samples were also reacted with α1–2 Fucosidase (10 U/μl; New England Biolabs) or O-glycanase (1.25 mU/μl; Prozyme, San Leandro, CA) as per the manufacturers' suggested protocols. The resultant protein samples were then separated on polyacrylamide gels, transferred onto nitrocellulose, and immunoblotted with our antibodies against either the cytoplasmic domain (anti-msAPPL-cyt) or extracellular domain (anti-msAPPL-ect) of msAPPL or with antibodies that had been pre-adsorbed against their peptide epitopes. Immunoblots that had been reacted with one antibody were routinely stripped and re-probed with the other antibody for an exact comparison of the protein bands recognized by antibodies specific for the different domains of msAPPL.

Results

The gene encoding msAPPL is developmentally expressed in the migratory EP cells

As an initial means of examining whether APPL-related proteins are expressed by the EP cells during their migration, we used an antiserum against *Drosophila* APPL (dAPPL) to immunostain embryos at 58% of development, a stage when the EP cells are still migrating but have also begun to extend axonal processes (see Fig. 1). Strong immunostaining was detected in all of the EP cells as they migrated onto the midgut muscle bands (Fig. 2A, arrows), including robust staining within their leading processes (Fig. 2A, arrowheads). To verify that these neurons express authentic APPL, we isolated a cDNA clone encoding the *Manduca* homologue of APPL (designated msAPPL; nucleotide and deduced amino acid sequences are shown in Supplemental Fig. 1). This cDNA clone contained a single open reading frame encoding a 732 AA protein that shares 51% overall sequence identity with dAPPL and 33% overall identity with human APP$_{695}$. The predicted structure of msAPPL is closely similar to other members of the APP family: it is a type-one transmembrane protein with several potential sites for N-linked glycosylation (see annotations in Supplemental Fig. 1). It also has the characteristic extracellular domains (E1 and E2) and cytoplasmic domain (C) found in all APP-related proteins (Bush et al., 1994; Coulson et al., 2000), although like dAPPL in *Drosophila* and APL-1 in *C. elegans*, msAPPL does not share sequence conservation with the Aβ region of human APP (Supplemental Fig. 2). msAPPL also lacks the large inserted sequences found between the E1 and E2 domains of *Drosophila* (Supplemental Fig. 2), so that the predicted molecular weight of its core protein (81 kDa) is closer to that of APP$_{695}$.

Sequence conservation between msAPPL and other APP-related proteins was found to be especially strong within its extracellular (E1 & E2) and cytoplasmic (C) domains (Fig. 2B). The E1 domain of msAPPL is 66% identical to that of dAPPL and 43% identical with human APP$_{695}$, while the E2 domain is 60% identical with that of dAPPL and 36% identical with APP$_{695}$. Of particular note is the high degree of sequence similarity between the cytoplasmic (C) domains of msAPPL and the equivalent domains in both fly (88%) and human APP$_{695}$ (77%), including a 100% conserved TPEERH sequence within the Goα binding domain of APP$_{695}$ (Nishimoto et al., 1993) and a 100% conserved NGYENPTYK sequence within the internalization motif required for interactions between APP$_{695}$ and the adapter proteins FE65, X11/Mint, and DAB1 (Turner et al., 2003).

To examine the expression pattern of msAPPL-specific mRNA, ^{32}P-labeled riboprobes were generated from our msAPPL cDNA clone and used in Northern blots of poly A$^+$ mRNA isolated from developing embryos. As shown in

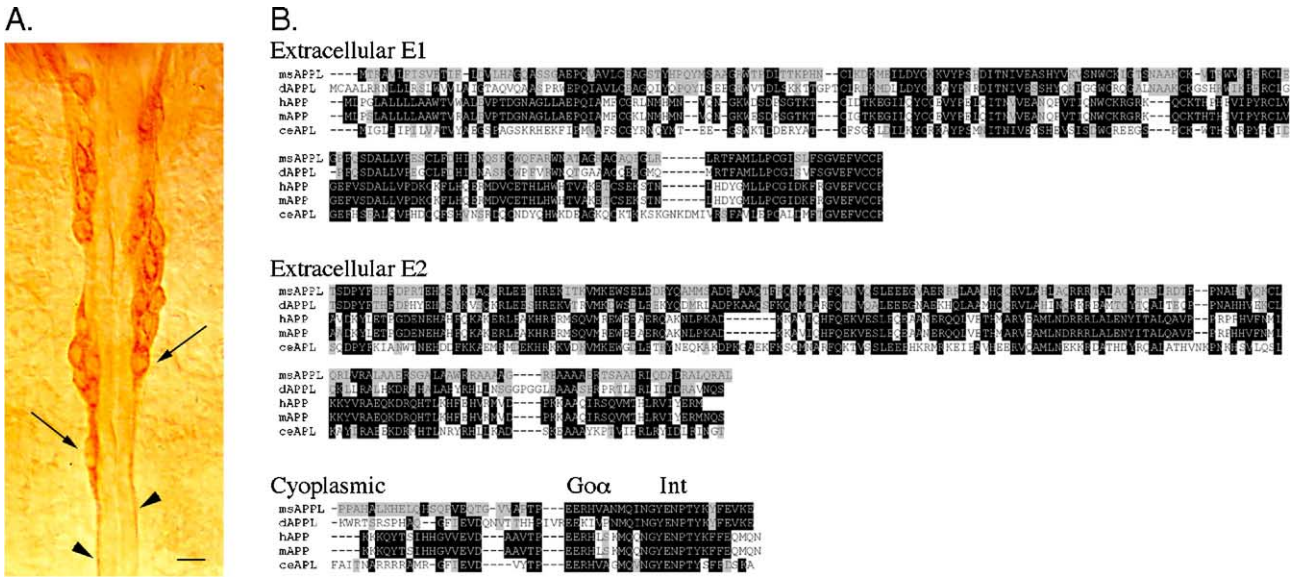

Fig. 2. The migratory EP cells express msAPPL, a member of the APP family. (A) Whole-mount preparation of a 58% embryo dissected to expose the migrating EP cells and immunostained with an antibody against dAPPL. Immunoreactivity can be clearly seen throughout the neuronal cell bodies (arrows) and in their leading processes (arrowheads) that are growing on the midgut muscle band pathways. Scale = 10 μm. (B) Amino acid alignment of conserved domains in msAPPL compared with *Drosophila* APPL (dAPPL), human APP_{695} (hAPP), mouse APP (mAPP), and *C. elegans* APL. Identical residues are shaded in black, similar residues are shaded in gray. Extracellular domains E1 and E2 represent putative protein interaction domains in the N-terminal regions of this protein family (see Supplemental Fig. 2 for schematic comparison of these structures). The C-terminal cytoplasmic domain contains the conserved putative binding site for Goα and an "internalization" motif (Int) that contains the binding sites for Fe65, X11/Mint, and DAB1 in vertebrate APPs. GenBank accession numbers for the sequences used in this alignment are #1303338A for human APP_{695}; #AAH70409 for mouse APP; #AAA28874 for *Drosophila* APPL; and #AAA98722 for *C. elegans* APL-1.

Fig. 3A, these probes recognized a single mRNA species at ~6.0 kb, similar to the 6.5 kb transcript reported for dAPPL mRNA (predicted to encode the slightly larger dAPPL protein; Rosen et al., 1989). Digoxigenin-labeled riboprobes were then used for in situ hybridization histochemical staining of staged embryos throughout the periods of EP cell neurogenesis, migration, and differentiation (Fig. 4). We previously showed that the EP cells first emerge from a neurogenic placode in the posterior dorsal lip of the foregut epithelium, a process that occurs between 30 and 40% of development (Copenhaver and Taghert, 1990). As shown in Fig. 4 (at 35% of development), no detectable msAPPL-specific mRNA was apparent in the EP cells during their initial delamination (arrows). In contrast, strong expression levels were apparent at this stage in neurons within the frontal ganglion on the anterior foregut (FrGl; arrowhead), which are born at an earlier period of development (Copenhaver and Taghert, 1991). By 40% of development, a stage when the EP cells are post-mitotic but have not yet begun to migrate (Copenhaver and Taghert, 1989b), faint levels of msAPPL mRNA could first be detected within the clustered neurons (Fig. 4, 40%). Staining intensities in the EP cells then steadily increased over the next 15% of development (40–55%), when the neurons spread circumferentially around the foregut–midgut boundary (black hatch marks in Fig. 4; see also Fig. 1 for orientation). All of the neurons continued to express robust levels of msAPPL-specific mRNA during their subsequent phase of fast migration onto the midgut muscle bands (Fig. 4, 55–65% of development; arrows indicate the progression of EP cell migration onto the mid-dorsal muscle bands). This pattern persisted throughout their subsequent periods of axon outgrowth (65–85%) and target innervation (75–100%; Copenhaver and Taghert, 1989a,b).

Elsewhere in the enteric nervous system, the expression levels of msAPPL mRNA remained high in all post-mitotic neurons that had migrated anteriorly along the course of the esophageal nerve (EN) to form the frontal ganglion (FrGl) and hypocerebral ganglion (HcGl) of the foregut (Fig. 5A). Throughout embryogenesis, strong msAPPL-specific staining was also detectable in neurons within the ganglia of the central nervous system (Fig. 5B) and in clusters of peripheral neurons on the body wall (Fig. 5B, arrowheads). In contrast, no detectable staining was seen in either central or peripheral glial cells nor in any other non-neural cell type within the embryo. These results indicate that msAPPL is a neuron-specific protein whose expression commences only after cells have completed their terminal mitosis. In the ENS, msAPPL expression in the EP cells coincides with the onset of their migratory behavior and persists throughout their subsequent phases of outgrowth and synapse formation.

msAPPL expression and processing are developmentally regulated in the ENS

In *Drosophila*, dAPPL has been shown to be expressed predominantly as a single glycosylated protein species of ~145 kDa, from which a ~130 kDa secreted fragment is rapidly processed by one or more secretase-like proteases (Luo et al., 1990). Immunoblots of protein extracted from the postembryonic CNS (Fig. 3B, lane 1) revealed a larger immunoreactive species at ~135 kDa and a smaller species at ~120 kDa. A

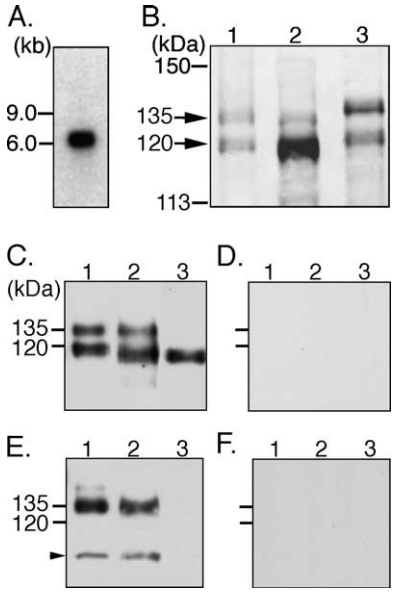

Fig. 3. Pattern of msAPPL-associated isoforms in the embryonic nervous system at the time of hatching (100% of development). (A) Northern blot of embryonic poly A^+ mRNA with a ^{32}P-labeled riboprobe specific for msAPPL revealed one prominent band at ~6.0 kb. (B) Immunoblot of protein extracts reacted with an antiserum against dAPPL, which recognizes a conserved motif in the ectodomain of msAPPL. Lane 1 = extract of *Manduca* larval CNS; lane 2 = extract from embryos at 100% of development; lane 3 = extract of *Drosophila* CNS. Arrows in panel B indicate the apparent size of full-length msAPPL (~135 kDa) and the secreted ectodomain (~120 kDa). (C) Neurons in primary culture express both the 135 and 120 kDa bands but secrete only the 120 kDa band into the surrounding culture medium. Immunoblot in panel C was labeled with our anti-msAPPL-ect antibody (against a peptide within the extracellular domain of msAPPL; see Supplemental Fig. 3). Lane 1 = extract of intact CNS; lane 2 = extract of primary neurons (isolated from pupal ganglia) after 6 days in culture; lane 3 = protein collected from the surrounding culture medium (harvested at the same time as the neurons); only the 120 kDa band was detected in the culture medium. (D) Identical immunoblot as shown in panel C that was labeled with an aliquot of the anti-msAPPL-ect antibody that had been pre-adsorbed against its specific peptide epitope. (E) Identical immunoblot as shown in panel C that was labeled with the anti-msAPPL-cyt antibody (against a peptide within the cytoplasmic domain of msAPPL; see Supplemental Fig. 3). This antibody detected the 135 kDa band but not the 120 kDa band in both CNS extracts (lane 1) and extracts from primary neurons (lane 2); no protein bands were labeled by this antibody in the medium sample (lane 3). The anti-msAPPL-cyt antibody also labels several larger bands in embryonic extracts that may represent isoforms of msAPPL with additional post-translational modifications (see Fig. 6); one of these bands is faintly detectable in lane 1 (above the 135 kDa band). A smaller band at ~117 kDa (arrowhead) detected by this antibody may represent a degradation product or an immature form of msAPPL. (F) Identical immunoblot as shown in panel E that was labeled with an aliquot of the anti-msAPPL-cyt antibody that had been pre-adsorbed against its specific peptide epitope. These results support the conclusion that the 135 kDa band represents the holoprotein (detected by both N- and C-terminal-specific msAPPL antibodies), while the 120 kDa band represents the secreted ectodomain (detected by the N-terminal but not the C-terminal-specific antibody) that is released from the surface of growing neurons.

similar pattern was seen in embryonic extracts (Fig. 3B, lane 2), although the 120 kDa band was substantially more abundant than 135 kDa band. As described below, this smaller 120 kDa band most likely represents the soluble ectodomain of msAPPL that is released after cleavage of the holoprotein by secretase activity, similar to the pattern seen in *Drosophila*. The apparent sizes of these proteins in *Manduca* are slightly smaller than those seen in *Drosophila* extracts (Fig. 3B, lane 3), as expected from the predicted amino acid sequences of the moth versus fly proteins (80 AA versus 98 AA; Luo et al., 1990) (see also Supplemental Fig. 2).

To examine whether the smaller 120 kDa band does represent the secreted ectodomain of msAPPL, we generated anti-peptide antibodies against specific sequences within the N- and C-terminal domains of the predicted protein (designated anti-msAPPL-ect and anti-msAPPL-cyt, respectively). The anti-msAPPL-ect antibody would be predicted to recognize both the holoprotein and any ectodomain fragments released by juxtamembrane secretase activity, while the anti-msAPPL-cyt antibody should recognize the holoprotein but not secreted ectodomains (see Supplemental Fig. 3). We then used primary cultures of *Manduca* CNS neurons to test whether the 120 kDa band was selectively released from the neurons into the surrounding medium. As shown in Fig. 3C, the anti-msAPPL-ect antibody recognized both the 135 kDa and 120 kDa bands in extracts prepared from intact CNS (lane 1) and in extracts of the primary neurons (lane 2; harvested 6 days after plating), but only the smaller 120 kDa band was detected in the surrounding medium (Fig. 3C, lane 3). All immunostaining was eliminated when we pre-adsorbed the antibody with the N-terminal domain peptide against which it was generated (Fig. 3D), whereas pre-adsorption of this antibody with the peptide used to generate the msAPPL-cyt antibody had no such effect (not shown).

In contrast, the anti-msAPPL-cyt antibody recognized only the larger 135 kDa band but not the 120 kDa band in extracts of both CNS (Fig. 3E, lane 1) and primary neurons (lane 2). This antibody also labeled several larger isoforms (discussed below) and a band at ~117 kDa (Fig. 3E, arrowhead), which may be an immature form of msAPPL or a degradation product. However, none of these bands were detected in the surrounding medium (Fig. 3E, lane 3). As with the N-terminal-specific antibody, pre-absorption of the anti-msAPPL-cyt antibody with its peptide epitope eliminated all detectable staining (Fig. 3F), whereas pre-adsorption with the peptide used to generate the anti-msAPPL-ect antibody had no effect (not shown). These results support the conclusion that the 120 kDa band detected with either the anti-dAPPL or anti-msAPPL-ect antibodies (both of which recognize epitopes in the extracellular regions of msAPPL) represents the secreted ectodomain of msAPPL, consistent with the release of the extracellular portions of other APP family proteins by juxtamembrane secretases (De Strooper and Annaert, 2000; Luo et al., 1990).

To examine the developmental expression of msAPPL over the course of embryonic development, we isolated body wall tissues (containing the CNS and PNS) and midgut tissue (containing the ENS) from embryos starting at 40% of embryogenesis, at which stage the EP cells have just begun to express the msAPPL gene. Equal amounts of total protein were then examined in immunoblots stained with antisera recognizing the N-terminal domain of msAPPL. In extracts of the body wall (Fig. 6A; containing protein from the CNS and PNS), msAPPL-related protein could be detected at 40% of

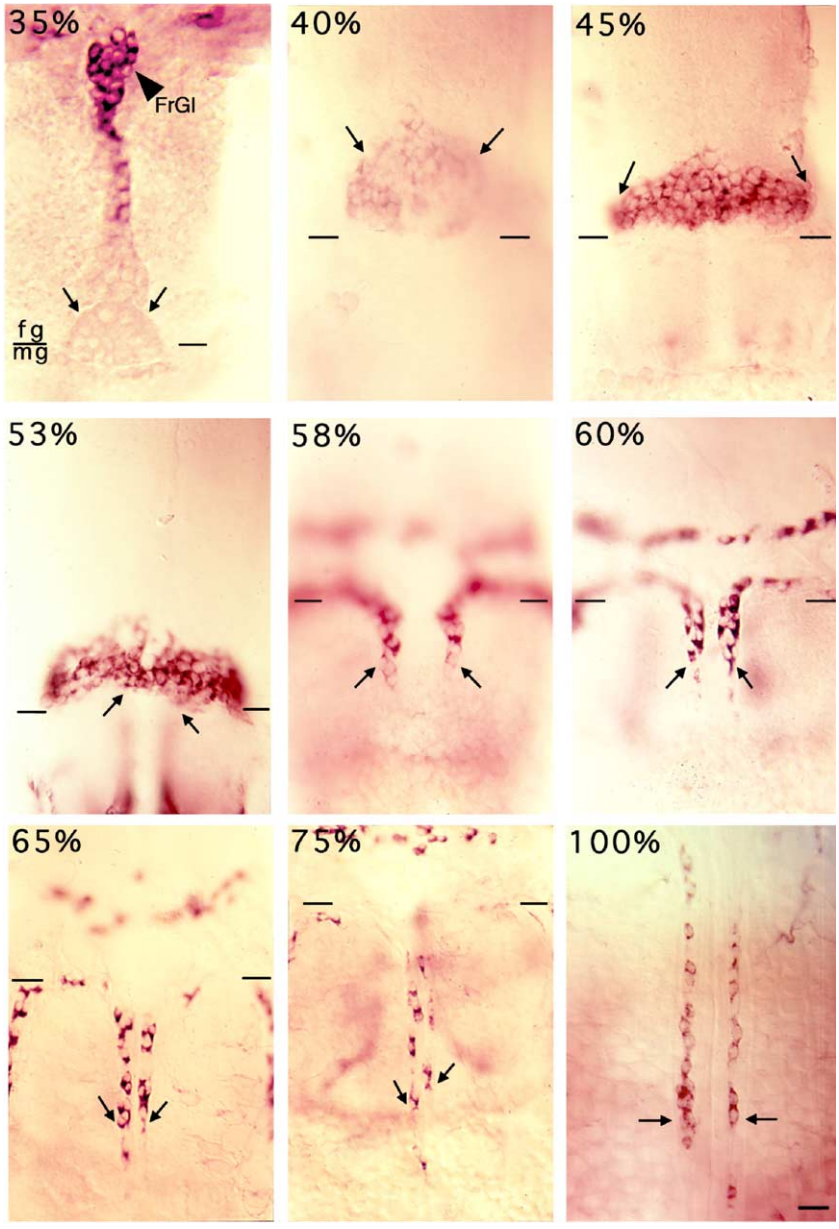

Fig. 4. Developmental expression of msAPPL mRNA in the EP cells. Whole-mount in situ hybridization histochemical staining of the ENS in embryos at progressive stages of development labeled with digoxigenin-labeled riboprobes against msAPPL mRNA. At 35%, the EP cells are still delaminating from a neurogenic placode (arrows) in the dorsal foregut lip and do not express detectable msAPPL mRNA; in contrast, neurons in the more anterior frontal ganglion (FrGl; born in an earlier wave of neurogenesis) express strong levels of msAPPL mRNA at this stage. By 40% of development, the EP cells form a coherent packet of post-mitotic neurons (arrows) on the dorsal foregut surface and express faint levels of msAPPL mRNA. Between 45 and 53%, the EP cells spread bilaterally around the foregut–midgut boundary and acquire strong expression levels of msAPPL mRNA. Between 53 and 55% of development, subsets of the EP cells align with the developing midgut muscle bands (arrows indicate positions of mid-dorsal muscle bands; compare with Fig. 1). Subsequently (from 55 to 65%), the neurons migrate posteriorly along the eight muscle bands onto the midgut. Arrows indicate progression of EP migration onto the mid-dorsal pair of band pathways (the dorsal four band pathways are visible in the 65% panel; compare with Fig. 1). High levels of msAPPL mRNA persist in the EP cells throughout their subsequent periods of axonal outgrowth (75–85%) and terminal differentiation (85–100% of development). Percentages indicate developmental stage of the embryos (in % of total embryogenesis). FrGl = frontal ganglion on the anterior foregut; black hatchmarks indicated the foregut–midgut boundary (fg/mg); scale bar = 30 μm.

development, corresponding to a period of active axonal and dendritic outgrowth by both central and peripheral neurons. Initially, both the 135 kDa and 120 kDa bands were of equal intensity, but, as development progressed, the 120 kDa band became markedly more intense (Fig. 6A, 65–85%). Given our data suggesting that the 120 kDa band represents the secreted ectodomain of msAPPL (Fig. 3), these results indicate that most of the protein expressed in the CNS was rapidly processed by one or more secretases during this period. However, by the completion of embryogenesis (100%), the relative abundance of the two isoforms had returned to approximately equal levels (as also shown in Fig. 3B, lane 1).

A similar trend was also detected in extracts containing proteins from the ENS (Fig. 6B). At 40% of development, soon after the onset of msAPPL expression by the EP cells (see Fig. 4), both the 135 kDa and 120 kDa isoforms could be detected

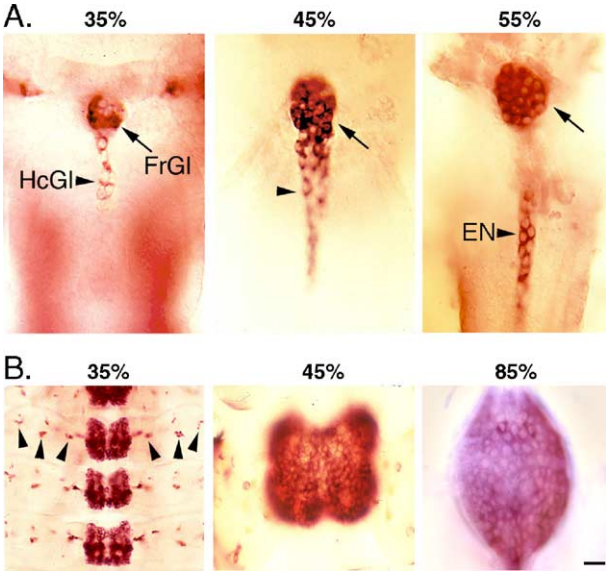

Fig. 5. Developmental expression of msAPPL mRNA in the ganglia of the ENS and CNS precedes that of the EP cells. (A) Whole-mount in situ hybridization histochemical staining of the foregut portion of the ENS shows strong levels of msAPPL gene expression in the neurons that migrate anteriorly to form the frontal ganglion (FrGl; arrow) and hypocerebral ganglion (HcGl; arrowhead; compare with Fig. 3, 35% of development). msAPPL-positive neurons continue to migrate into the hypocerebral ganglion via the developing esophageal nerve (EN) throughout the first half of embryogenesis. (B) Expression of msAPPL mRNA is also clearly detectable at 35% of development in neurons within the ganglia of the CNS and in the peripheral neurons of the body wall (arrowheads); expression levels remain high in the CNS throughout the remainder of embryonic development. FrGl = frontal ganglion; HcGl = hypocerebral ganglion; EN = esophageal nerve of the foregut. Scale bar = 15 μm in panel B, 35%, and 40 μm in all other panels.

in extracts containing these neurons. In addition, however, we also detected three larger bands with apparent molecular weights of 155–180 kDa (Fig. 6B, arrowheads) that were not seen in postembryonic tissue extracts. These larger protein species remained abundant throughout subsequent phases of EP cell migration (55–65%) and outgrowth (70–85%), while the 135 kDa band was reduced in relative intensity throughout much of this period. Only towards the end of embryogenesis did the 135 kDa band become more apparent. By 100% of development (hatching), the higher molecular weight bands were no longer detectable, leaving only the 135 kDa and 120 kDa bands (as seen in the CNS).

Previous studies have shown that both human APP_{695} and fly dAPPL isoforms are often glycosylated (Weidemann et al., 1989; Luo et al., 1990), and, as noted above, the predicted sequence for msAPPL includes at least three potential sites for N-linked glycosylation, as well as potential sites for O-glycosylation and fucosylation (Supplemental Fig. 1). To test whether the larger protein species seen in Fig. 6B (arrowheads) might represent hyperglycosylated isoforms of msAPPL, we reacted embryonic lysates with PNGase F to remove N-linked glycoproteins (Plummer and Tarentino, 1991) and then examined them in immunoblots labeled with a combination of our anti-msAPPL antibodies to reveal all potential isoforms. When we used embryo extracts prepared in RIPA buffer, we found that both the 135 kDa and 120 kDa bands (putatively the full-length and secreted ectodomains of msAPPL) were shifted to lower apparent molecular sizes by 3–4 kDa (compare lanes 2 and 3 in Fig. 6C), consistent with the effects of perturbing endoglycosylation in other APP family proteins (Luo et al., 1990; Oltersdorf et al., 1990). A larger shift was seen in the apparent sizes of the higher molecular weight bands, each being reduced by ~10–12 kDa. When we prepared embryonic lysates with hot extraction buffer (as per the manufacturer's suggestion), we also observed the 155–180 kDa trio of bands plus the 135 and 120 kDa isoforms (Fig. 6C, lane 4). However, treatment of this preparation with PNGase completely eliminated the higher molecular weight bands, while the intensity of the 135 kDa band was enhanced (Fig. 6C, lane 5), suggesting that the higher molecular weight isoforms might represent hyperglycosylated forms of full-length msAPPL. In contrast,

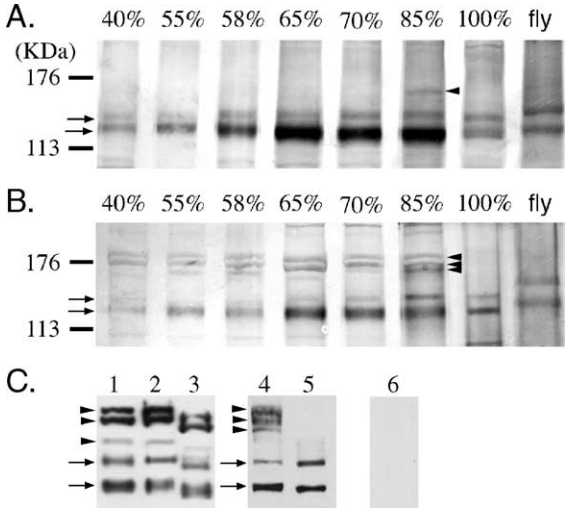

Fig. 6. Immunoblot analysis of the developmental expression and processing of msAPPL in the CNS and ENS. (A) Extracts of the embryonic body wall (containing the embryonic CNS and peripheral neurons); (B) extracts of the foregut–midgut region (containing the developing EP cells and their processes). Paired arrows to the left of the blots indicate the position of full-length msAPPL (135 kDa) and the secreted ectodomain (120 kDa). Black arrowheads indicate the higher molecular weight isoforms (155–180 kDa) that are present in the EP cells during their phases of migration and outgrowth (40–85% of development; also faintly seen at 85% in panel A). (C) Treatment of msAPPL in embryonic lysates with the deglycosylating enzyme PNGase F. Blots were labeled with a combination of our anti-msAPPL-cyt and anti-msAPPL-ect antibodies to reveal all detectable isoforms of msAPPL. Lane 1 = control sample of embryonic lysate prepared in RIPA buffer; arrows indicate the 135 and 120 kDa bands, arrowheads indicate the 155–180 trio of higher molecular weight bands. Lane 2 = embryonic lysate incubated overnight in PNGase buffer but without PNGase; no artifactual degradation of the msAPPL-associated bands was detected. Lane 3 = identical sample reacted overnight in PNGase buffer plus PNGase; the large trio of bands (155–180 kDa) was reduced in apparent size by ~10–12 kDa, while the 135 and 120 kDa bands were reduced by 3–4 kDa. Lane 4: embryo lysate prepared in hot extraction buffer (see Materials and methods) and incubated overnight in PNGase buffer without PNGase. Lane 5: identical sample as in Lane 4 reacted with PNGase; the trio of higher molecular weight bands (arrowheads) was eliminated by this treatment, while the 135 kDa band was enhanced in intensity. However, the 135 and 120 kDa bands exhibited only minimal changes in their apparent size. Lane 6: an identical sample of embryonic lysate as shown in lane 1 that was labeled with anti-msAPPL antibodies that had been pre-adsorbed against their peptide epitopes; all detectable immunolabeled bands were eliminated by the pre-adsorption protocol.

only minimal reductions were seen in the size of the 135 and 120 kDa bands with this treatment. Pre-incubation of the antisera with their peptide epitopes eliminated labeling of the trio of higher molecular weight proteins as well as the 135 and 120 kDa isoforms, (Fig. 6C, lane 6; compare with lane 1).

Because the residual size of the deglycosylated bands in either of these reaction conditions was still substantially larger than the predicted mass of the core protein of msAPPL (~81 kDa), we also reacted embryo extracts with O-glycanase (to remove O-linked glycoproteins) or α1–2 Fucosidase (to remove fucosyl side groups); however, neither of these treatments further reduced the apparent size of the msAPPL isoforms (not shown). Additional modifications that may contribute to this discrepancy in size are discussed below. Nevertheless, these results indicate that msAPPL undergoes a dynamic sequence of post-translational modification and processing in the EP cells over the course of their migration and subsequent differentiation.

Developmental trafficking of msAPPL during EP cell differentiation

To gain a better understanding of how msAPPL is distributed in the EP cells during their migration, we immunostained identically staged embryos either with antibodies against the cell adhesion receptor fasciclin II (mFas II; to show the full extent of EP cell outgrowth; Wright et al., 1999) or with our anti-APPL antibodies. A third set of matched preparations was stained with an antibody against ELAV (Robinow and White, 1991), an unambiguous neuronal marker that we have shown labels the EP cells but not enteric glial cells (Copenhaver, 1993). As previously described (Copenhaver and

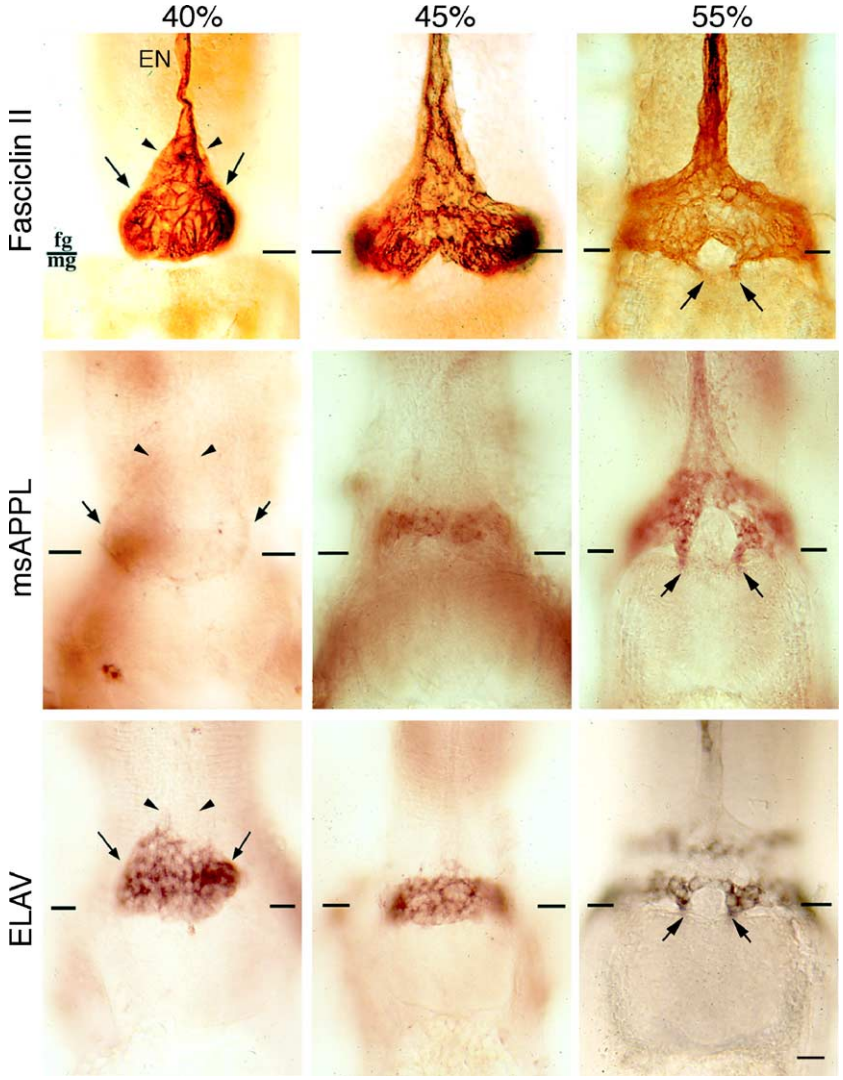

Fig. 7. Expression of msAPPL protein in the EP cells during their slow spreading phase of development (40–55% of embryogenesis). Identically staged embryos (40, 45, and 55% of development) were immunostained as whole-mount preparations either with antibodies against *Manduca* fasciclin II (top row), APPL (middle row), or ELAV (bottom row). Arrows at 40% indicate the initial position of the EP cell packet on the foregut before the onset of the lateral spreading phase of migration; arrowheads indicate the anterior cluster of associated glial precursors that do not express msAPPL or ELAV. Arrows at 55% of development indicate the EP cell clusters that have begun to align with the mid-dorsal pair of muscle bands (compare with Fig. 4). Black hatchmarks indicate the foregut–midgut boundary (fg/mg); EN = esophageal nerve of the foregut. Scale bar = 30 μm.

Taghert, 1990), when the EP cells first delaminate onto the foregut, they form a packet of post-mitotic but pre-migratory neurons (Fig. 7, arrows) positioned adjacent to a rostral cluster of glial precursor cells (arrowheads) that are associated with the esophageal nerve (EN). By 40% of development, all of the EP cells had begun to express ELAV; in contrast, msAPPL expression was not detectable in these neurons until several hours later, first appearing in the EP cells as they commenced their slow circumferential spreading phase of migration around the foregut (Fig. 7, 40–55% of development). Like ELAV, msAPPL expression was restricted to the neurons of the ENS, being absent from the enteric glia or underlying visceral musculature. Throughout this period of development, msAPPL immunoreactivity was distributed in a punctate manner throughout the cytoplasm of the EP cells, as well as within their short filopodial processes extending on the adjacent foregut and midgut surfaces (described below). Subsequently, during their fast phase of migration onto the midgut muscle bands (55–65% of development; Fig. 8), all of the EP cells continued to express robust levels of APPL-related protein. As with mFas II, msAPPL immunoreactivity could be clearly seen in their leading processes and growing axons (Fig. 8, arrows), in contrast to ELAV, which was largely confined to the neuronal cell bodies.

The co-localization of msAPPL with mFas II was better demonstrated in confocal images of preparations that had

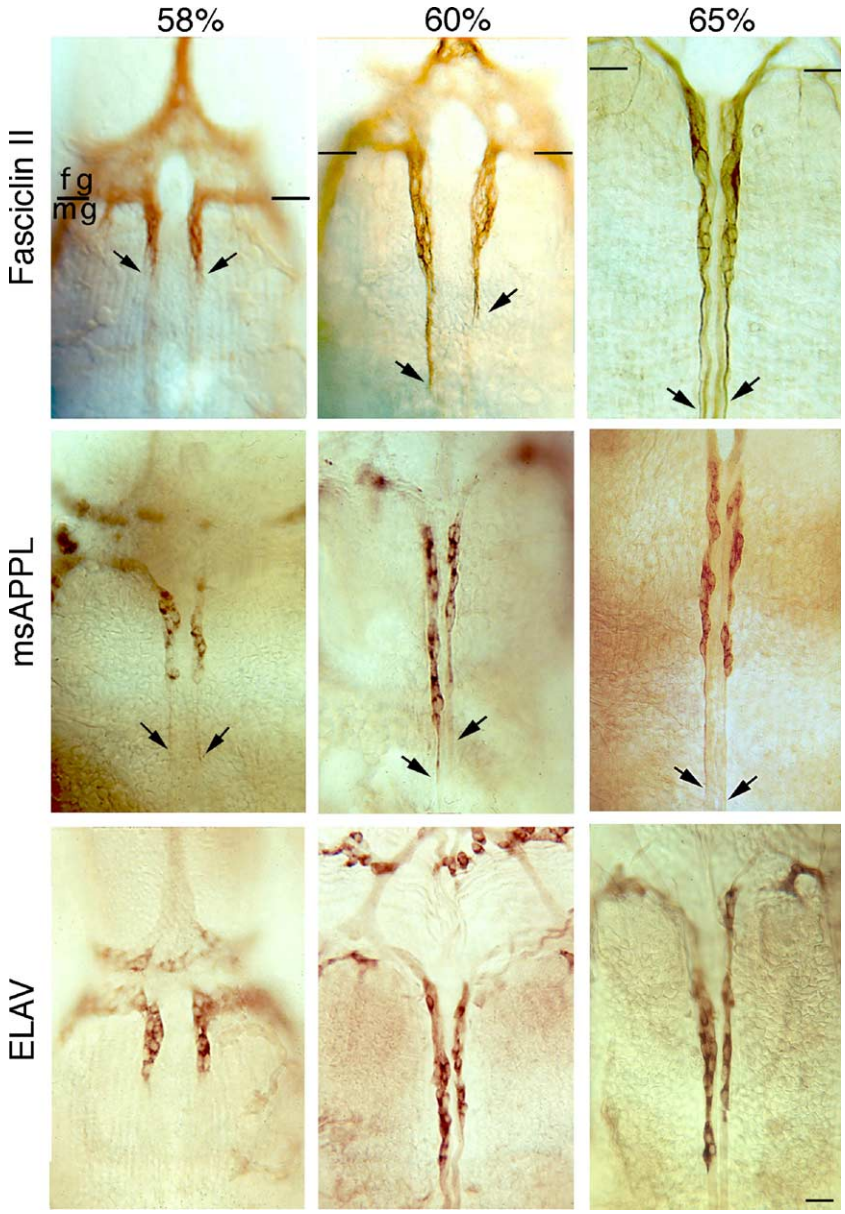

Fig. 8. msAPPL continues to be expressed by the EP cells during their migration onto the midgut muscle bands and can be detected within their leading processes. Identically staged embryos (58, 60, and 65% of development) were immunostained as whole-mount preparations with antibodies to fasciclin II (top row), APPL (middle row), or ELAV (bottom row). Arrows indicate the leading processes of the EP cells (at 58% and 60%) or their growing axons (at 65%) that extended along the mid-dorsal set of muscle bands; compare with Fig. 4. In contrast, ELAV in *Manduca* is restricted to the neuronal somata. Black bars indicate the foregut–midgut boundary (fg/mg); scale bar = 30 μm.

been double-labeled with antibodies against these two proteins (Fig. 9). In actively migrating neurons (Fig. 9A; 58% of development), mFas II immunostaining (red) defined the outline of the EP cells (arrows) and their leading processes (arrowheads) and more faintly labeled their underlying muscle band pathways (asterisks; as described in Wright and Copenhaver, 2000). During this phase of migration, robust APPL immunoreactivity (green) was associated with the leading processes of the EP cells (Fig. 9A, arrowheads), as well as a more diffuse pattern of punctate staining throughout their somata (arrows). At higher magnification (Fig. 9B, different preparation than in panel A), co-localization of msAPPL and mFas II could clearly be seen within filopodia of leading processes of the EP cells (arrowheads); intriguingly, msAPPL was distributed all the way to the tips of some filopodia but not others, suggesting that the trafficking of this protein is dynamically regulated in these highly motile structures.

By 95% of development (Fig. 9C), a stage when the EP cells have completed their differentiation (see Fig. 1), the distributions of both proteins had changed substantially. mFas II immunoreactivity was primarily localized to the axons of the EP cells that had grown around the cell bodies of neighboring neurons, although some of this staining was associated with the enteric glial cells that ensheath the EP cell bodies (Wright and Copenhaver, 2000). APPL immunoreactivity was also still expressed in the axons of the EP cells (Fig. 9C) and could be faintly detected in their diffuse terminal branches on the interband musculature (not shown). However, the cytoplasmic component of msAPPL was now confined to a ring of large perinuclear vesicles that did not contain mFas II (Fig. 9C, arrows). These results indicate that, in addition to the developmentally regulated processing of msAPPL shown in Fig. 6, msAPPL (or its proteolytic fragments) undergoes differential trafficking in the EP cells, coincident with the different stages of neuronal migration and differentiation.

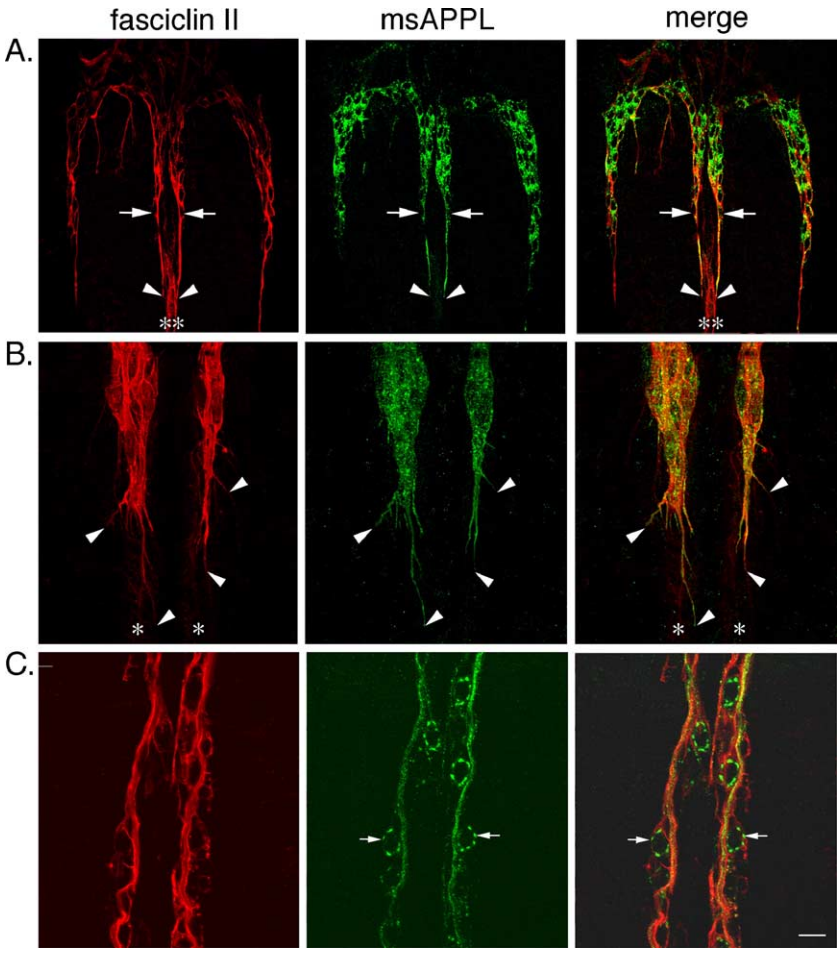

Fig. 9. msAPPL undergoes developmentally regulated trafficking within the migratory EP cells. Confocal images of embryos double-immunostained for fasciclin II (red) and msAPPL (green). (A) In actively migrating EP cells (58% of development), msAPPL immunoreactivity is distributed in a punctate manner throughout the cytoplasm of the EP cells and also co-localizes with mFas II in their leading processes (arrowheads); white arrows indicate positions of the leading EP cells on each mid-dorsal muscle band pathway. (B) Higher magnification view of the migrating EP cells and their leading processes in a 58% embryo (different preparation than in panel A) shows that msAPPL immunoreactivity is distributed to the tips of some filopodia associated with their leading processes (arrowheads) but only spreads partially out the length of others. Asterisks indicate the position of mid-dorsal pair of muscle bands, which also express faint levels of mFas II (Wright and Copenhaver, 2000). (C) In differentiated EP cells (95% of development), some msAPPL still co-localizes with the fasciculated axons of the EP cells, but most of the cytoplasmic msAPPL immunoreactivity is confined to a perinuclear ring of vesicles within the neuronal somata (arrows). Scale bar = 30 μm in row A and 15 μm in rows B and C.

msAPPL interacts with the heterotrimeric G protein Goα in the migratory EP cells

Previously, we showed that the EP cells first express the gene encoding the heterotrimeric G protein Goα just prior to the onset of migration (Horgan et al., 1995) and that Goα is the only G protein detectable in the leading processes of these neurons during their subsequent migration and outgrowth (Horgan et al., 1994, 1995). Since human APP_{695} has been shown to interact directly with Goα in vertebrate cells (Brouillet et al., 1999; Nishimoto et al., 1993), we used confocal imaging of embryos that had been double-labeled with antibodies against msAPPL and Goα to examine the relative distributions of these two proteins in vivo. As shown in Fig. 10A, the two proteins were spatially co-localized within both the somata (arrows) and growing axons (arrowheads) of the EP cells. Goα is also transiently expressed by the midline cells (ml) lying between the muscle band pathways that are followed by the migratory neurons (Horgan et al., 1994), but these midline cells were devoid of msAPPL expression.

Because of relatively high background levels associated with our anti-Goα antibody in whole-mount preparations, we were unable to resolve the fine filopodial processes of the EP cells in these preparations. As an alternative strategy, we immunostained neurons grown in primary culture (3 days after plating) for msAPPL and Goα. As shown in Figs. 10B–C, the distribution of the two proteins largely overlapped within the major neurites and finer filopodial extensions of cultured neurons undergoing active outgrowth. These results indicate that msAPPL and Goα are co-localized in the motile regions of both central and peripheral neurons in *Manduca*.

To test whether msAPPL and Goα interact within the EP cells, we immunoprecipitated msAPPL from extracts of embryonic midgut and probed the immunoprecipitate with the anti-Goα antibody. As shown in Fig. 11A, the initial midgut extracts ("input") contained a substantial amount of Goα.

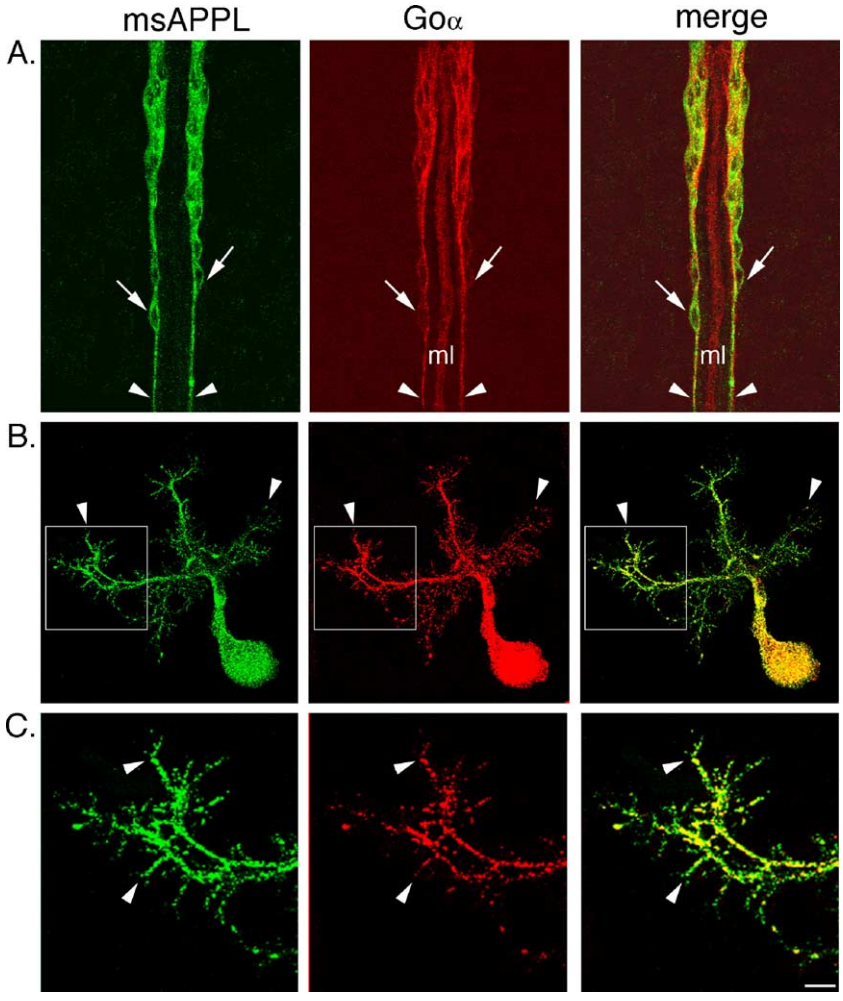

Fig. 10. (A) Co-localization of msAPPL and the heterotrimeric G protein Goα in the migratory EP cells. Embryo at 60% of development immunostained with antibodies against msAPPL (green) and Goα (red). Arrows indicate the leading neurons on the two mid-dorsal muscle bands; arrowheads indicate their leading processes that have begun to elongate into incipient axons. (B) Co-localization of msAPPL and Goα in a cultured primary neuron (3 days after plating). Arrowheads indicate growing neurites containing both msAPPL and Goα immunoreactivity. (C) Magnified views of the boxed regions indicated in panel B. ml = midline cells between the mid-dorsal muscle bands that also express Goα but not msAPPL at 58% of development. Scale bar = 15 μm in panel A, 5 μm in panel B, and 2 μm in panel C.

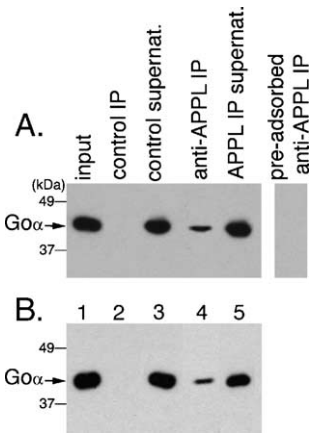

Fig. 11. Goα co-immunoprecipitates with msAPPL. (A) Immunoblot of proteins derived from embryonic midgut and labeled with an anti-Goα antiserum. Input = a control sample of the midgut lysate, showing that it contains robust levels of Goα. Control IP = proteins that were immunoprecipitated with pre-immune sera (from the chicken used to generate our anti-msAPPL-cyt antibody); no detectable Goα was seen in this sample, while the residual supernatant from this immunoprecipitation reaction ("control supernatant") contained similar Goα levels as seen in the initial lysate (compare with the "input" lane). In contrast, incubation of the midgut lysate with our anti-msAPPL-cyt antibody co-immunoprecipitated Goα ("anti-APPL IP"); approximately 10% of the total Goα in the initial lysate was co-precipitated by this protocol. Residual levels of Goα (not co-precipitated by anti-msAPPL) are shown in "anti-APPL supernatant." No detectable Goα was seen when lysates were incubated with an aliquot of the anti-msAPPL antibody that had been pre-adsorbed against its peptide epitope ("pre-adsorbed anti-APPL IP"). (B) Co-immunoprecipitation of Goα with msAPPL from lysates of desheathed pupal ganglia (used to prepare our primary neuronal cultures; see Fig. 10). Lanes are identical to those in panel A: lane 1 = input (ganglia lysate); lane 2 = control immunoprecipitate (using pre-immune sera); lane 3 = residual supernatant from the control immunoprecipitation shown in lane 2; lane 4 = immunoprecipitate using anti-msAPPL antibodies, which contains about 10% of the total Goα seen in the initial lysate (compare with lane 1); lane 5 = residual supernatant from the immunoprecipitation reaction shown in lane 4. The size of Goα (41 kDa) is indicated on the left of each panel.

When we immunoprecipitated this extract with pre-immune sera, no detectable Goα was seen in the precipitated protein pellet ("control IP"). In contrast, when we immunoprecipitated midgut extract with either of our anti-msAPPL antibodies, approximately 10% of the total amount of Goα that was detectable in the original lysate co-immunoprecipitated with msAPPL ("anti-APPL IP"). Pre-incubation of the anti-msAPPL antibodies with their peptide epitopes completely abolished their ability to co-immunoprecipitate Goα ("pre-adsorbed anti-APPL IP"). In a parallel study, we also co-immunoprecipitated msAPPL and Goα from lysates of desheathed CNS ganglia (isolated by the same protocol used for preparing our primary neuronal cultures; see Fig. 10). As with the embryonic midgut extracts, extracts of CNS ganglia contained robust levels of Goα (Fig. 11B, lane 1). Pre-immune serum failed to co-immunoprecipitate any detectable Goα (Fig. 11B, lane 2), whereas our anti-msAPPL antisera immunoprecipitated approximately 10% of the total Goα (Fig. 11B, lane 4) detectable in the initial ganglia lysate. Neither of our anti-msAPPL antibodies co-precipitated the related G protein Gsα (not shown), providing further evidence that the interaction between msAPPL and Goα is specific.

These results show that msAPPL and Goα are closely associated in *Manduca* neurons. Moreover, since the EP cells are the only cells on the midgut that express detectable levels of both msAPPL (Figs. 7–8) and Goα (Horgan et al., 1995), these experiments indicate that msAPPL interacts with Goα specifically in these migratory neurons. In combination with our previous demonstration that Goα-mediated signaling inhibits EP cell migration in vivo (Horgan and Copenhaver, 1998), our data support a model whereby interactions between msAPPL and Goα may regulate specific aspects of neuronal migration, as discussed below.

Discussion

A potential role for APPL in the regulation of migration by Goα

In previous work, we presented evidence that activation of Goα in the EP cells negatively regulates their motile behavior: Goα is expressed in the EP cells coincident with the onset of their migration (Horgan et al., 1994) and activation of Goα within individual EP cells leads to an inhibition of their migration and outgrowth (Horgan and Copenhaver, 1998; Horgan et al., 1994). This inhibitory effect of Goα was shown to be mediated by Ca^{2+} influx via voltage-independent channels; moreover, G protein activation induces the onset of intrinsic Ca^{2+} spiking activity in the EP cells and results in a down-regulation of their motility (Horgan and Copenhaver, 1998). Spontaneous Ca^{2+} spikes of similar amplitude can be detected in the EP cells at the end of their migration, supporting the conclusion that Goα-dependent activation of Ca^{2+} influx normally regulates the guidance or extent of EP cell migration and outgrowth along the midgut muscle bands (Horgan and Copenhaver, 1998). Based on these results, we proposed a model whereby Goα-coupled receptors expressed by the EP cells would be activated by ligands encountered within the local cellular environment, resulting in the stimulation of Goα-mediated Ca^{2+} spiking activity in the EP cells and a concomitant regulation of their migratory behavior (Horgan and Copenhaver, 1998). However, the identity of candidate receptors capable of activating Goα in these neurons remained unknown.

The results described in current study suggest that msAPPL, a member of the APP family of transmembrane proteins, may serve this function. Our data show that msAPPL and Goα are co-localized within the EP cells during their migration and within the growing processes of neurons in primary culture (Fig. 10). We have also shown that Goα can be co-immunoprecipitated with anti-msAPPL antibodies from extracts of both the ENS and CNS (Fig. 11). Given the high degree of sequence similarity between the Goα binding domain of human APP_{695} (Nishimoto et al., 1993) and the equivalent domain in msAPPL (Fig. 2), these results are consistent with the proposal that msAPPL and Goα directly interact in the EP cells.

A hypothetical model supported by our data is that msAPPL acts as an atypical Goα-coupled receptor in the EP cells that

regulates their response to inhibitory guidance cues in a Goα-dependent manner (Fig. 12). In previous work, we showed that the EP cells extend filopodial processes onto both the muscle band pathways (B) and the adjacent interband regions (IB), areas that are inhibitory to migration (Copenhaver et al., 1996). Filopodia that extend onto the interband regions are significantly shorter and have briefer lifespans than those that grow along the muscle bands (unpublished observations), supporting the notion that ligands (Fig. 12, red) encountered within the interband regions may induce a local retraction response. By the proposed model, binding of these ligands by msAPPL would induce the local activation of Goα and Ca^{2+} influx in filopodia growing onto the interbands, leading to their retraction; msAPPL-dependent activation of Goα would therefore serve to restrict the migration and outgrowth of the EP cells to their permissive muscle band pathways. Alternatively, more global activation of this signaling cascade within an EP cell would inhibit its overall migration, a response that might help regulate the normal distribution of these neurons to the anterior segment of the midgut (Copenhaver and Taghert, 1989a,b). As with APP_{695}, authentic ligands for msAPPL remain unknown, but they might include either membrane-associated molecules or secreted factors derived from interband cells, both of which would be readily accessible to msAPPL in the leading processes of the EP cells.

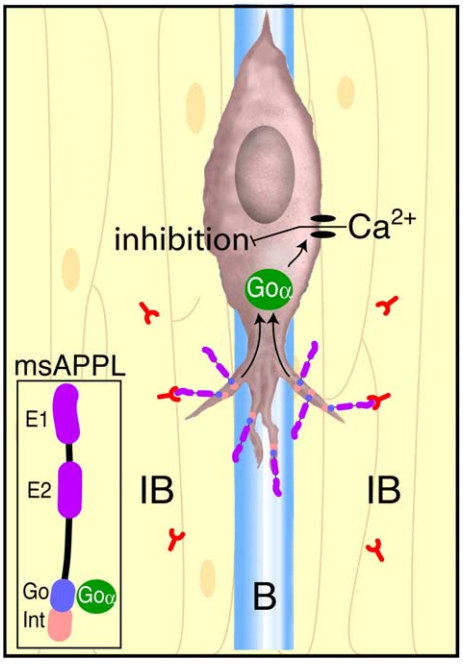

Fig. 12. A model for the regulation of EP cell migration via msAPPL-dependent activation of Goα. An EP cell that is migrating on a midgut muscle band (B; blue) also extends multiple filopodia onto the adjacent interband regions of the midgut (IB), which are inhibitory to migration. msAPPL (purple) co-localizes with Goα in the leading processes of the migratory neurons, where it is transiently oriented as a transmembrane receptor. An interaction between specific ligands for msAPPL (red) on the interband cells would lead to local activation of Goα within the EP cell, which in turn has been shown to trigger the induction of Ca^{2+} spiking activity in migrating EP cells and an inhibition of their motility (Horgan and Copenhaver, 1998). By this model, local activation of Goα following msAPPL activation would induce the retraction of filopodia from the interband regions, while global activation would result in a termination of EP cell migration (and possibly lead to subsequent aspects of neuronal differentiation; Copenhaver and Taghert, 1989b). This model can now be tested by interfering with msAPPL expression in the EP cells (which should induce ectopic migration) and by examining whether activation of msAPPL leads to the induction of Goα-sensitive Ca^{2+} spiking activity.

Support for this model may be inferred from a variety of studies in other systems. APP-related proteins are expressed in high levels within in the leading processes and growth cones of motile neurons in all species examined (Moya et al., 1994; Lahiri et al., 2002; Clarris et al., 1995; Ohta et al., 1993), and experiments in cell culture have shown that APP (or its proteolytic derivatives) can modulate neuronal motility and outgrowth in a variety of contexts (Kibbey et al., 1993; Beher et al., 1996; Perez et al., 1997; Qiu et al., 1995). Although an authentic role for human APP_{695} in the developing nervous system remains controversial, a recent study on triple-knockout mice lacking APP and the related genes APLP1 and APLP2 revealed a dramatic defect in neuronal migratory behavior: subsets of cortical neurons in these mice failed to recognize their normal cues to terminate migration, resulting in aberrant migration through the overlying pial layer (Herms et al., 2004). Similarly, a recent examination of developing neuromuscular junctions in mice lacking both APP and APLP2 revealed that these animals exhibit defective synaptic structures associated with excessive nerve terminal sprouting (Wang et al., 2005). In preliminary studies, we recently found that inhibition of msAPPL expression (using msAPPL-specific morpholino probes) resulted in excessive, inappropriate migration by the EP cells onto the normally inhibitory interband regions of the midgut, consistent with the model shown in Fig. 12 (Copenhaver et al., unpublished data). Although in both mice and *Manduca*, the cues that are recognized by APP-related molecules remain to be determined, these results support the hypothesis that members of the APP family may act as transmembrane receptors involved in the regulation of neuronal migratory behavior and outgrowth.

Precedent for our model that msAPPL may act as a novel Goα-coupled receptor can also be found in studies on human APP_{695}. Nishimoto et al. showed that Goα (but not other G proteins) binds directly to a cytoplasmic domain of APP_{695} containing a TPEERH motif (Nishimoto et al., 1993), an amino acid sequence that is 100% conserved in *Manduca* msAPPL (Fig. 2). Moreover, activation of APP_{695} with an antibody against its ectodomain induced a significant increase in GTPγS turnover by Goα, analogous to G protein activation by conventional G-protein-coupled receptors (Nishimoto et al., 1993; Okamoto et al., 1995). This same group showed that one class of APP_{695} mutations linked to Familial AD caused these proteins to act as constitutively active Goα-linked receptors when incorporated into vesicles (Okamoto et al., 1996) or in cultured cells (Ikezu et al., 1996). The direct interaction between APP_{695} and Goα was verified in other experiments using neuronal membranes (Brouillet et al., 1999), although, in this study, activation of APP_{695} caused an *inhibition* of Goα GTPase activity, underscoring the challenges of working with isolated membrane preparations. Nevertheless, these studies advanced the provocative model that APP may act as a novel

type of G protein-coupled receptor that regulates Goα activity, although the downstream signaling events that may be modulated by APP proteins remain undefined (Turner et al., 2003). Our demonstration that msAPPL interacts with Goα in the EP cells provides a model system that can now be used to test the role of this APP family protein in regulating neuronal motility, specifically via the modulation of Ca^{2+} spiking activity in vivo; these experiments are currently underway.

Relationship of msAPPL to other APP family proteins

As noted above, msAPPL shares most of the major structural features found in other APP family proteins, including conserved motifs in both the extracellular and intracellular domains that have been implicated in a variety of potential interactions with other proteins (Fig. 2; Supplemental Fig. 2; De Strooper and Annaert, 2000; Turner et al., 2003). Like "neuronal" APP_{695} and fly dAPPL (Rosen et al., 1989), msAPPL lacks the KPI domain found in the larger APP isoforms that are expressed in non-neuronal cells (Turner et al., 2003). Both *Manduca* and *Drosophila* APLPs are expressed exclusively in neurons (Figs. 4–6; Martin-Morris and White, 1990), although they lack obvious homology with the Aβ region of human APP_{695}. In this regard, the insect versions of this protein more closely resemble the vertebrate APLPs, which have been postulated to have arisen along with APP via gene duplication from a single ancestral gene (Coulson et al., 2000).

Our data also indicate that, like human APP_{695} (Walter et al., 2001) and fly dAPPL (Luo et al., 1990), msAPPL is expressed as a glycosylated transmembrane protein that is rapidly processed to produce a smaller secreted ectodomain fragment. In the CNS, the holoprotein appears primarily as a 135 kDa protein that can be processed by secretase-like activity to produce a soluble 120 kDa fragment. As shown in Fig. 3, we were able to detect this 120 kDa fragment but not the 135 kDa protein in the medium of cultured primary neurons, using our antibody against the N-terminal domain of msAPPL but not with our C-terminal-specific antibody. These data support our conclusion that the 120 kDa protein represents the cleaved ectodomain fragment of the holoprotein. Notably, we only detected the 120 kDa protein in the medium surrounding the neurons after several days in culture, suggesting that continued expression and cleavage of msAPPL lead to the gradual accumulation of this fragment as the neurons grow. Other bands recognized by our C-terminal-specific antibody (including the 135 kDa isoform) were not detected in the medium, nor was the 120 kDa band seen in control samples of the culture medium (not shown). We also obtained analogous results when we expressed msAPPL in *Drosophila* S2 cells, similar to previous published studies by Luo et al. on dAPPL (Luo et al., 1990), albeit with somewhat altered apparent molecular weights (unpublished data). These results support the conclusion that msAPPL undergoes secretase-dependent processing in a manner similar to that of other APP family members. Although the specific identity of the secretases responsible for msAPPL processing in *Manduca* have yet to be verified, we have now isolated cDNAs encoding evolutionarily conserved members of all of the α-, β-, and γ-secretase families implicated in APP_{695} processing (De Strooper and Annaert, 2000). In future work, we intend to investigate how secretase-dependent cleavage of msAPPL affects different aspects of EP cell motility in vivo.

Dynamic features of msAPPL expression during migration

Several aspects of msAPPL expression in the EP cells may pertain to its potential role as a guidance receptor involved in modulating neuronal migration. First, expression of msAPPL-specific mRNA (Fig. 4) and protein (Fig. 7) was initially detected in the EP cells just prior to the onset of their slow spreading phase of development, several hours after the completion of their terminal mitoses (Copenhaver and Taghert, 1990) and after the onset of ELAV expression (Fig. 7). These results are consistent with the delayed expression of dAPPL in the *Drosophila* CNS, which is detectable only after the expression of other neuronal-specific markers (Martin-Morris and White, 1990). Because the EP cells are the only neurons on the midgut during embryogenesis, immunoblots of this tissue provided an accurate view of msAPPL processing in the EP cells at different stages of their development (Fig. 6B). Notably, during periods of active migration and outgrowth, much of the msAPPL associated with the EP cells appeared to undergo extensive post-translational modification, resulting in the three prominent bands at 155–180 kDa. By the completion of embryogenesis, these larger isoforms were no longer apparent, so that virtually all of the full-length proteins migrated at 135 kDa (as seen in extracts of the CNS). These results suggest that stage-specific regulation of post-translational processing events may contribute to the developmental role of msAPPL in actively motile neurons.

The nature of the modifications that contribute to the apparent size of these larger isoforms remains incompletely understood. As shown in Fig. 6C, PNGase F treatment of lysates prepared with hot extraction buffer suggested that the trio of bands at 155–180 kDa may be hyperglycosylated forms of full-length APPL; however, this protocol failed to shift the apparent size of the 135 and 120 kDa proteins, which is inconsistent with published reports that both the holoprotein and secreted ectodomains of APP proteins are glycosylated (Luo et al., 1990; Oltersdorf et al., 1990). In contrast, PNGase treatment of lysates prepared in RIPA buffer did shift these bands by 3–4 kDa but only reduced the larger trio of bands by 10–15 kDa. Our hot extraction protocol might possibly sensitize carbohydrate side chains on msAPPL that are normally resistant to PNGase treatment, although treatments with O-glycanase and Fucosidase had no effect on any of the msAPPL-associated bands. APP family proteins are also subject to phosphorylation (Russo et al., 2005) and sumoylation (Li et al., 2003), but such modifications should not be affected by the protocols used in this study. Alternatively, the higher molecular weight bands might be due in part to homodimerization of msAPPL isoforms, as has been suggested for human APP_{695} (Scheuermann et al., 2001). In such a case,

the combination of hot extraction buffer and PNGase treatment might have serendipitously disrupted potential homophilic interactions, resulting in the shift in apparent molecular weights that we observed.

Although the significance of these different aspects of msAPPL processing remain to be explored in terms of the control of neuronal migration, these results suggest that the post-translational modification and rapid turnover of transmembrane msAPPL may play important roles in regulating the distribution and bioavailability of the holomolecule or its proteolytic fragments. For example, studies performed with rat neuronal membranes showed that only a small fraction of intact APP was accessible to the extracellular space at any given time, but that this same fraction co-localized with Goα and was responsible for modulating GTPγS turnover when activated by antibody cross-linking (Brouillet et al., 1999). Consistent with this view, immunostaining unpermeabilized preparations of the ENS with our anti-msAPPL antibodies resulted in a greatly diminished signal compared to that seen in fixed permeabilized embryos (unpublished observations), indicating that the holoprotein of msAPPL may reside on the surface of growing neurons only briefly before being proteolytically cleaved. This pattern of rapid expression and processing of a potential guidance receptor might provide a means of continually refreshing a neuron's response to dynamic changes in the extracellular cues that it encounters during its migration into the ENS. In this regard, the distribution of msAPPL on the leading processes of the migrating EP cells is intriguing, in that we observed that msAPPL extended into the distal tips of some filopodia but not others (Fig. 9). In the context of our proposed model, msAPPL may preferentially traffic to filopodia that are undergoing active elongation and are therefore most likely to encounter potential ligands in the local environment; alternatively, the protein might accumulate in filopodia that have become stabilized and are forming focal contacts, as has been suggested from studies of mouse APP in transfected cells and primary neuronal cultures (Sabo et al., 2001, 2003).

Lastly, while msAPPL expression remained strong in the EP cells throughout their differentiation, we noted a marked redistribution of the protein as the neurons matured. During their active phase of migration, msAPPL was distributed in a punctate manner throughout the EP cells, consistent with the vesicular trafficking of APP by fast anterograde transport (Lazarov et al., 2005; Stokin et al., 2005). In addition, a fraction of msAPPL also co-localized with mFas II (Fig. 9) and Goα (Fig. 10) in the leading processes and axons of the EP cells in vivo and CNS neurons grown in primary culture, lending credence to our model that msAPPL-dependent activation of Goα plays a role in migratory guidance. By the end of embryogenesis, however, most msAPPL within the somata of the EP cells was confined to a ring of large perinuclear vesicles (Fig. 9C), although some of the proteins remained associated with the axonal fascicles and terminal branches of these neurons. While the identity of these perinuclear vesicles is still unknown, they resemble the intracellular compartments in which vertebrate APPs (or their derivatives) have been shown to accumulate (Lee et al., 2003; Nixon et al., 2000; Takahashi et al., 2004), which may be endosomal or lysosomal in nature.

These results suggest that msAPPL may be differentially trafficked during EP cell development so that membrane-associated msAPPL is concentrated in regions of active motility and target innervation, while much of the remaining protein or its processed fragments become localized within this perinuclear compartment. Although cytoplasmic fragments of human APP_{695} have been shown to be capable of trafficking to the nucleus and regulating gene transcription (Kinoshita et al., 2002; but see Cao and Sudhof, 2004), the pattern of sequestration that we observed at the completion of migration and outgrowth would also provide an effective means of limiting the capacity of msAPPL to modulate Goα activity. In summary, our data indicate that in actively migrating EP cells, msAPPL undergoes a dynamic sequence of post-translational modification, trafficking, and processing, consistent with the view that this protein may play an important role in regulating one or more aspects of directed neuronal migration in this system.

Acknowledgments

We wish to thank Drs. Vivian Budnik, Mary Packard, and Kalpana White for generously sharing their anti-dAPPL antibodies and Dr. Budnik for many fruitful discussions on the biology of APPL. We also wish to thank Drs. Michael Forte and Doris Kretzschmar for critical evaluations of this work. Dr. Stefani Kaech-Petrie (of the Live Cell Imaging Facility in the Center for Research in Occupational and Environmental Toxicology) and Aurelie Snyder (of the OHSU-MMI Research Core Facility; (http://www.ohsu.edu/core) provided invaluable assistance in the generation of several of our confocal images. Ms. Kesley Mauch provided valuable technical assistance in performing primary neuronal cultures. Dr. Tiffani Howard (tiffani@howardink.com) produced the excellent graphics shown in Fig. 12 and Supplemental Figs. 2 and 3. This work was supported in part by NIH # NS34439 to PFC, by NIH P30 AG08017, and a grant from the Oregon Partnership for Alzheimer's Research. The GenBank accession number for msAPPL is DQ008058.

Appendix A. Supplementary data

Supplementary data associated with this article can be found in the online version at doi:10.1016/j.ydbio.2005.09.029.

References

Akaaboune, M., Allinquant, B., Farza, H., Roy, K., Magoul, R., Fiszman, M., Festoff, B.W., Hantai, D., 2000. Developmental regulation of amyloid precursor protein at the neuromuscular junction in mouse skeletal muscle. Mol. Cell. Neurosci. 15, 355–367.

Annaert, W., De Strooper, B., 2002. A cell biological perspective on Alzheimer's disease. Annu. Rev. Cell Dev. Biol. 18, 25–51.

Ashley, J., Packard, M., Ataman, B., Budnik, V., 2005. Fasciclin II signals new synapse formation through amyloid precursor protein and the scaffolding protein dX11/Mint. J. Neurosci. 25, 5943–5955.

Beher, D., Hesse, L., Masters, C.L., Multhaup, G., 1996. Regulation of amyloid protein precursor (APP) binding to collagen and mapping of the binding sites on APP and collagen type I. J. Biol. Chem. 271, 1613–1620.

Brouillet, E., Trembleau, A., Galanaud, D., Volovitch, M., Bouillot, C., Valenza, C., Prochiantz, A., Allinquant, B., 1999. The amyloid precursor protein interacts with Go heterotrimeric protein within a cell compartment specialized in signal transduction. J. Neurosci. 19, 1717–1727.

Bush, A.I., Pettingell Jr., W.H., de Paradis, M., Tanzi, R.E., Wasco, W., 1994. The amyloid beta-protein precursor and its mammalian homologues. Evidence for a zinc-modulated heparin-binding superfamily. J. Biol. Chem. 269, 26618–26621.

Cao, X., Sudhof, T.C., 2004. Dissection of amyloid-beta precursor protein-dependent transcriptional transactivation. J. Biol. Chem. 279, 24601–24611.

Chen, M., Yankner, B.A., 1991. An antibody to beta amyloid and the amyloid precursor protein inhibits cell–substratum adhesion in many mammalian cell types. Neurosci. Lett. 125, 223–226.

Clarris, H.J., Key, B., Beyreuther, K., Masters, C.L., Small, D.H., 1995. Expression of the amyloid protein precursor of Alzheimer's disease in the developing rat olfactory system. Brain Res. Dev. Brain Res. 88, 87–95.

Copenhaver, P.F., 1993. Origins, migration, and differentiation of glial cells in the insect nervous system from a discrete set of glial precursors. Development 117, 59–74.

Copenhaver, P.F., Taghert, P.H., 1988. Position-dependent expression of peptidergic phenotype in post-migratory neurons of the insect enteric system. Abstr. -Soc. Neurosci. 14, 770.

Copenhaver, P.F., Taghert, P.H., 1989a. Development of the enteric nervous system in the moth I. Diversity of cell types and the embryonic expression of FMRFamide-related neuropeptides. Dev. Biol. 131, 70–84.

Copenhaver, P.F., Taghert, P.H., 1989b. Development of the enteric nervous system in the moth II. Stereotyped cell migration precedes the differentiation of embryonic neurons. Dev. Biol. 131, 85–101.

Copenhaver, P.F., Taghert, P.H., 1990. Neurogenesis in the insect enteric nervous system: generation of pre-migratory neurons from an epithelial placode. Development 109, 17–28.

Copenhaver, P.F., Taghert, P.H., 1991. Origins of the insect enteric nervous system: differentiation of the enteric ganglia from a neurogenic epithelium. Development 113, 1115–1132.

Copenhaver, P.F., Horgan, A.M., Combes, S., 1996. An identified set of visceral muscle bands is essential for the guidance of migratory neurons in the enteric nervous system of *Manduca sexta*. Dev. Biol. 179, 412–426.

Coulson, E.J., Paliga, K., Beyreuther, K., Masters, C.L., 2000. What the evolution of the amyloid protein precursor supergene family tells us about its function. Neurochem. Int. 36, 175–184.

Daigle, I., Li, C., 1993. apl-1, a *Caenorhabditis* elegans gene encoding a protein related to the human beta-amyloid protein precursor. Proc. Natl. Acad. Sci. U. S. A. 90, 12045–12049.

De Strooper, B., Annaert, W., 2000. Proteolytic processing and cell biological functions of the amyloid precursor protein. J. Cell Sci. 113 (Pt. 11), 1857–1870.

Edmond, B.T., Moomaw, C.R., Hsu, J.T., Slaughter, C., Ellis, L., 1990. The p38 and p34 polypeptides of growth cone particle membranes are the α and b subunits of G proteins. Dev. Brain Res. 56, 131–136.

Giambarella, U., Yamatsuji, T., Okamoto, T., Matsui, T., Ikezu, T., Murayama, Y., Levine, M.A., Katz, A., Gautam, N., Nishimoto, I., 1997. G protein betagamma complex-mediated apoptosis by familial Alzheimer's disease mutant of APP. EMBO J. 16, 4897–4907.

Glenner, G.G., Wong, C.W., 1984. Alzheimer's disease: initial report of the purification and characterization of a novel cerebrovascular amyloid protein. Biochem. Biophys. Res. Commun. 120, 885–890.

Greeve, I., Kretzschmar, D., Tschape, J.A., Beyn, A., Brellinger, C., Schweizer, M., Nitsch, R.M., Reifegerste, R., 2004. Age-dependent neurodegeneration and Alzheimer-amyloid plaque formation in transgenic *Drosophila*. J. Neurosci. 24, 3899–3906.

Gunawardena, S., Goldstein, L.S., 2001. Disruption of axonal transport and neuronal viability by amyloid precursor protein mutations in *Drosophila*. Neuron 32, 389–401.

Hardy, J., Allsop, D., 1991. Amyloid deposition as the central event in the aetiology of Alzheimer's disease. Trends Pharmacol. Sci. 12, 383–388.

Hardy, J., Selkoe, D.J., 2002. The amyloid hypothesis of Alzheimer's disease: progress and problems on the road to therapeutics. Science 297, 353–356.

Hayashi, J.H., Hildebrand, J.G., 1990. Insect olfactory neurons in vitro: morphological and physiological characterization of cells from the developing antennal lobes of *Manduca sexta*. J. Neurosci. 10, 848–859.

Hayashi, J.H., Levine, R.B., 1992. Calcium and potassium currents in leg motoneurons during postembryonic development in the hawkmoth *Manduca sexta*. J. Exp. Biol. 171, 15–42.

Heber, S., Herms, J., Gajic, V., Hainfellner, J., Aguzzi, A., Rulicke, T., von Kretzschmar, H., von Koch, C., Sisodia, S., Tremml, P., Lipp, H.P., Wolfer, D.P., Muller, U., 2000. Mice with combined gene knock-outs reveal essential and partially redundant functions of amyloid precursor protein family members. J. Neurosci. 20, 7951–7963.

Herms, J., Anliker, B., Heber, S., Ring, S., Fuhrmann, M., Kretzschmar, H., Sisodia, S., Muller, U., 2004. Cortical dysplasia resembling human type 2 lissencephaly in mice lacking all three APP family members. EMBO J. 23, 4106–4115.

Horgan, A.M., Copenhaver, P.F., 1998. G protein-mediated inhibition of neuronal migration requires calcium influx. J. Neurosci. 18, 4189–4200.

Horgan, A.M., Lagrange, M.T., Copenhaver, P.F., 1994. Developmental expression of G proteins in a migratory population of embryonic neurons. Development 120, 729–742.

Horgan, A.M., Lagrange, M.T., Copenhaver, P.F., 1995. A developmental role for the heterotrimeric G protein Go_{α} in a migratory population of embryonic neurons. Dev. Biol. 172, 640–653.

Ikezu, T., Okamoto, T., Komatsuzaki, K., Matsui, T., Martyn, J.A., Nishimoto, I., 1996. Negative transactivation of cAMP response element by familial Alzheimer's mutants of APP. EMBO J. 15, 2468–2475.

Kamenetz, F., Tomita, T., Hsieh, H., Seabrook, G., Borchelt, D., Iwatsubo, T., Sisodia, S., Malinow, R., 2003. APP processing and synaptic function. Neuron 37, 925–937.

Kang, J., Lemaire, H.G., Unterbeck, A., Salbaum, J.M., Masters, C.L., Grzeschik, K.H., Multhaup, G., Beyreuther, K., Muller-Hill, B., 1987. The precursor of Alzheimer's disease amyloid A4 protein resembles a cell-surface receptor. Nature 325, 733–736.

Kibbey, M.C., Jucker, M., Weeks, B.S., Neve, R.L., Van Nostrand, W.E., Kleinman, H.K., 1993. Beta-amyloid precursor protein binds to the neurite-promoting IKVAV site of laminin. Proc. Natl. Acad. Sci. U. S. A. 90, 10150–10153.

Kinoshita, A., Whelan, C.M., Berezovska, O., Hyman, B.T., 2002. The gamma secretase-generated carboxyl-terminal domain of the amyloid precursor protein induces apoptosis via Tip60 in H4 cells. J. Biol. Chem. 277, 28530–28536.

Kirazov, E., Kirazov, L., Bigl, V., Schliebs, R., 2001. Ontogenetic changes in protein level of amyloid precursor protein (APP) in growth cones and synaptosomes from rat brain and prenatal expression pattern of APP mRNA isoforms in developing rat embryo. Int. J. Dev. Neurosci. 19, 287–296.

Kitaguchi, N., Takahashi, Y., Tokushima, Y., Shiojiri, S., Ito, H., 1988. Novel precursor of Alzheimer's disease amyloid protein shows protease inhibitory activity. Nature 331, 530–532.

Klein, W.L., 2002. Abeta toxicity in Alzheimer's disease: globular oligomers (ADDLs) as new vaccine and drug targets. Neurochem. Int. 41, 345–352.

Lahiri, D.K., Nall, C., Chen, D., Zaphiriou, M., Morgan, C., Nurnberger Sr., J.I., 2002. Developmental expression of the beta-amyloid precursor protein and heat-shock protein 70 in the cerebral hemisphere region of the rat brain. Ann. N. Y. Acad. Sci. 965, 324–333.

Lazarov, O., Morfini, G.A., Lee, E.B., Farah, M.H., Szodorai, A., DeBoer, S.R., Koliatsos, V.E., Kins, S., Lee, V.M., Wong, P.C., Price, D.L., Brady, S.T., Sisodia, S.S., 2005. Axonal transport, amyloid precursor protein, kinesin-1, and the processing apparatus: revisited. J. Neurosci. 25, 2386–2395.

Lee, M.S., Kao, S.C., Lemere, C.A., Xia, W., Tseng, H.C., Zhou, Y., Neve, R., Ahlijanian, M.K., Tsai, L.H., 2003. APP processing is regulated by cytoplasmic phosphorylation. J. Cell Biol. 163, 83–95.

Li, H.L., Roch, J.M., Sundsmo, M., Otero, D., Sisodia, S., Thomas, R., Saitoh, T., 1997. Defective neurite extension is caused by a mutation in amyloid beta/A4 (A beta) protein precursor found in familial Alzheimer's disease. J. Neurobiol. 32, 469–480.

Li, Y., Wang, H., Wang, S., Quon, D., Liu, Y.W., Cordell, B., 2003. Positive and negative regulation of APP amyloidogenesis by sumoylation. Proc. Natl. Acad. Sci. U. S. A. 100, 259–264.

Li, Y., Liu, T., Peng, Y., Yuan, C., Guo, A., 2004. Specific functions of *Drosophila* amyloid precursor-like protein in the development of nervous system and nonneural tissues. J. Neurobiol. 61, 343–358.

Loffler, J., Huber, G., 1992. Beta-amyloid precursor protein isoforms in various rat brain regions and during brain development. J. Neurochem. 59, 1316–1324.

Luo, L.Q., Martin-Morris, L.E., White, K., 1990. Identification, secretion, and neural expression of APPL, a *Drosophila* protein similar to human amyloid protein precursor. J. Neurosci. 10, 3849–3861.

Luo, L., Tully, T., White, K., 1992. Human amyloid precursor protein ameliorates behavioral deficit of flies deleted for Appl gene. Neuron 9, 595–605.

Martin-Morris, L.E., White, K., 1990. The *Drosophila* transcript encoded by the beta-amyloid protein precursor-like gene is restricted to the nervous system. Development 110, 185–195.

Masliah, E., Mallory, M., Ge, N., Saitoh, T., 1992. Amyloid precursor protein is localized in growing neurites of neonatal rat brain. Brain Res. 593, 323–328.

Masters, C.L., Simms, G., Weinman, N.A., Multhaup, G., McDonald, B.L., Beyreuther, K., 1985. Amyloid plaque core protein in Alzheimer disease and Down syndrome. Proc. Natl. Acad. Sci. U. S. A. 82, 4245–4249.

Moya, K.L., Benowitz, L.I., Schneider, G.E., Allinquant, B., 1994. The amyloid precursor protein is developmentally regulated and correlated with synaptogenesis. Dev. Biol. 161, 597–603.

Mucke, L., Masliah, E., Johnson, W.B., Ruppe, M.D., Alford, M., Rockenstein, E.M., Forss-Petter, S., Pietropaolo, M., Mallory, M., Abraham, C.R., 1994. Synaptotrophic effects of human amyloid beta protein precursors in the cortex of transgenic mice. Brain Res. 666, 151–167.

Nishimoto, I., Okamoto, T., Matsaura, Y., Takahashi, S., 1993. Alzheimer amyloid protein precursor complexes with brain GTP-binding protein Go. Nature 362, 75–79.

Nixon, R.A., Cataldo, A.M., Mathews, P.M., 2000. The endosomal–lysosomal system of neurons in Alzheimer's disease pathogenesis: a review. Neurochem. Res. 25, 1161–1172.

Ohta, M., Kitamoto, T., Iwaki, T., Ohgami, T., Fukui, M., Tateishi, J., 1993. Immunohistochemical distribution of amyloid precursor protein during normal rat development. Brain Res. Dev. Brain Res. 75, 151–161.

Okamoto, T., Takeda, S., Murayama, Y., Ogata, E., Nishimoto, I., 1995. Ligand-dependent G protein coupling function of amyloid transmembrane precursor. J. Biol. Chem. 270, 4205–4208.

Okamoto, T., Takeda, S., Giambarella, U., Murayama, Y., Matsui, T., Katada, T., Matsuura, Y., Nishimoto, I., 1996. Intrinsic signaling function of APP as a novel target of three V642 mutations linked to familial Alzheimer's disease. EMBO J. 15, 3769–3777.

Oltersdorf, T., Ward, P.J., Henriksson, T., Beattie, E.C., Neve, R., Lieberburg, I., Fritz, L.C., 1990. The Alzheimer amyloid precursor protein. Identification of a stable intermediate in the biosynthetic/degradative pathway. J. Biol. Chem. 265, 4492–4497.

Patel, N.H., Goodman, C.S., 1992. DIG-labeled single-stranded DNA probes for in situ hybridization. In: Kessler, C. (Ed.), Non-Radioactive Labelling and Detection of Biomolecules. Springer, Heidelberg, pp. 377–381.

Perez, R.G., Zheng, H., Van der Ploeg, L.H., Koo, E.H., 1997. The beta-amyloid precursor protein of Alzheimer's disease enhances neuron viability and modulates neuronal polarity. J. Neurosci. 17, 9407–9414.

Plummer Jr., T.H., Tarentino, A.L., 1991. Purification of the oligosaccharide-cleaving enzymes of *Flavobacterium meningosepticum*. Glycobiology 1, 257–263.

Qiu, W.Q., Ferreira, A., Miller, C., Koo, E.H., Selkoe, D.J., 1995. Cell-surface beta-amyloid precursor protein stimulates neurite outgrowth of hippocampal neurons in an isoform-dependent manner. J. Neurosci. 15, 2157–2167.

Robinow, S., White, K., 1991. Characterization and spatial distribution of the ELAV protein during *Drosophila melanogaster* development. J. Neurobiol. 22, 443–461.

Rosen, D.R., Martin-Morris, L., Luo, L.Q., White, K., 1989. A Drosophila gene encoding a protein resembling the human beta-amyloid protein precursor. Proc. Natl. Acad. Sci. U. S. A. 86, 2478–2482.

Russo, C., Venezia, V., Repetto, E., Nizzari, M., Violani, E., Carlo, P., Schettini, G., 2005. The amyloid precursor protein and its network of interacting proteins: physiological and pathological implications. Brain Res. Brain Res. Rev. 48, 257–264.

Sabo, S.L., Ikin, A.F., Buxbaum, J.D., Greengard, P., 2001. The Alzheimer amyloid precursor protein (APP) and FE65, an APP-binding protein, regulate cell movement. J. Cell Biol. 153, 1403–1414.

Sabo, S.L., Ikin, A.F., Buxbaum, J.D., Greengard, P., 2003. The amyloid precursor protein and its regulatory protein, FE65, in growth cones and synapses in vitro and in vivo. J. Neurosci. 23, 5407–5415.

Sandbrink, R., Masters, C.L., Beyreuther, K., 1994a. Beta A4-amyloid protein precursor mRNA isoforms without exon 15 are ubiquitously expressed in rat tissues including brain, but not in neurons. J. Biol. Chem. 269, 1510–1517.

Sandbrink, R., Masters, C.L., Beyreuther, K., 1994b. Similar alternative splicing of a non-homologous domain in beta A4-amyloid protein precursor-like proteins. J. Biol. Chem. 269, 14227–14234.

Scheuermann, S., Hambsch, B., Hesse, L., Stumm, J., Schmidt, C., Beher, D., Bayer, T.A., Beyreuther, K., Multhaup, G., 2001. Homodimerization of amyloid precursor protein and its implication in the amyloidogenic pathway of Alzheimer's disease. J. Biol. Chem. 276, 33923–33929.

Selkoe, D.J., 1998. The cell biology of beta-amyloid precursor protein and presenilin in Alzheimer's disease. Trends Cell Biol. 8, 447–453.

Selkoe, D.J., 2000. Toward a comprehensive theory for Alzheimer's disease. Hypothesis: Alzheimer's disease is caused by the cerebral accumulation and cytotoxicity of amyloid beta-protein. Ann. N.Y. Acad. Sci. 924, 17–25.

Selkoe, D.J., 2001. Alzheimer's disease: genes, proteins, and therapy. Physiol. Rev. 81, 741–766.

Stern, E.A., Bacskai, B.J., Hickey, G.A., Attenello, F.J., Lombardo, J.A., Hyman, B.T., 2004. Cortical synaptic integration in vivo is disrupted by amyloid-beta plaques. J. Neurosci. 24, 4535–4540.

Stokin, G.B., Lillo, C., Falzone, T.L., Brusch, R.G., Rockenstein, E., Mount, S.L., Raman, R., Davies, P., Masliah, E., Williams, D.S., Goldstein, L.S., 2005. Axonopathy and transport deficits early in the pathogenesis of Alzheimer's disease. Science 307, 1282–1288.

Struble, R.G., Dhanraj, D.N., Mei, Y., Wilson, M., Wang, R., Ramkumar, V., 1998. Beta-amyloid precursor protein-like immunoreactivity is upregulated during olfactory nerve regeneration in adult rats. Brain Res. 780, 129–137.

Suh, Y.H., Checler, F., 2002. Amyloid precursor protein, presenilins, and alpha-synuclein: molecular pathogenesis and pharmacological applications in Alzheimer's disease. Pharmacol. Rev. 54, 469–525.

Takahashi, R.H., Almeida, C.G., Kearney, P.F., Yu, F., Lin, M.T., Milner, T.A., Gouras, G.K., 2004. Oligomerization of Alzheimer's beta-amyloid within processes and synapses of cultured neurons and brain. J. Neurosci. 24, 3592–3599.

Tong, L., Balazs, R., Thornton, P.L., Cotman, C.W., 2004. Beta-amyloid peptide at sublethal concentrations downregulates brain-derived neurotrophic factor functions in cultured cortical neurons. J. Neurosci. 24, 6799–6809.

Torroja, L., Chu, H., Kotovsky, I., White, K., 1999a. Neuronal overexpression of APPL, the *Drosophila* homologue of the amyloid precursor protein (APP), disrupts axonal transport. Curr. Biol. 9, 489–492.

Torroja, L., Packard, M., Gorczyca, M., White, K., Budnik, V., 1999b. The *Drosophila* beta-amyloid precursor protein homolog promotes synapse differentiation at the neuromuscular junction. J. Neurosci. 19, 7793–7803.

Turner, P.R., O'Connor, K., Tate, W.P., Abraham, W.C., 2003. Roles of amyloid precursor protein and its fragments in regulating neural activity, plasticity and memory. Prog. Neurobiol. 70, 1–32.

von Koch, C.S., Zheng, H., Chen, H., Trumbauer, M., Thinakaran, G., van der Ploeg, L.H., Price, D.L., Sisodia, S.S., 1997. Generation of APLP2 KO mice and early postnatal lethality in APLP2/APP double KO mice. Neurobiol. Aging 18, 661–669.

Walsh, D.M., Klyubin, I., Fadeeva, J.V., Cullen, W.K., Anwyl, R., Wolfe, M.S., Rowan, M.J., Selkoe, D.J., 2002. Naturally secreted oligomers of amyloid beta protein potently inhibit hippocampal long-term potentiation in vivo. Nature 416, 535–539.

Walter, J., Kaether, C., Steiner, H., Haass, C., 2001. The cell biology of Alzheimer's disease: uncovering the secrets of secretases. Curr. Opin. Neurobiol. 11, 585–590.

Wang, P., Yang, G., Mosier, D.R., Chang, P., Zaidi, T., Gong, Y.D., Zhao, N.M., Dominguez, B., Lee, K.F., Gan, W.B., Zheng, H., 2005. Defective neuromuscular synapses in mice lacking amyloid precursor protein (APP) and APP-like protein 2. J. Neurosci. 25, 1219–1225.

Wasco, W., Bupp, K., Magendantz, M., Gusella, J.F., Tanzi, R.E., Solomon, F., 1992. Identification of a mouse brain cDNA that encodes a protein related to the Alzheimer disease-associated amyloid beta protein precursor. Proc. Natl. Acad. Sci. U. S. A. 89, 10758–10762.

Wasco, W., Gurubhagavatula, S., Paradis, M.D., Romano, D.M., Sisodia, S.S., Hyman, B.T., Neve, R.L., Tanzi, R.E., 1993. Isolation and characterization of APLP2 encoding a homologue of the Alzheimer's associated amyloid beta protein precursor. Nat. Genet. 5, 95–100.

Weidemann, A., Konig, G., Bunke, D., Fischer, P., Salbaum, J.M., Masters, C.L., Beyreuther, K., 1989. Identification, biogenesis, and localization of precursors of Alzheimer's disease A4 amyloid protein. Cell 57, 115–126.

Wright, J.W., Copenhaver, P.F., 2000. Different isoforms of fasciclin II play distinct roles in the guidance of neuronal migration during insect embryogenesis. Dev. Biol. 225, 59–78.

Wright, J.W., Copenhaver, P.F., 2001. Cell type-specific expression of fasciclin II isoforms reveals neuronal–glial interactions during peripheral nerve growth. Dev. Biol. 234, 24–41.

Wright, J.W., Schwinof, K.M., Snyder, M.A., Copenhaver, P.F., 1998. A delayed role for nitric oxide-sensitive guanylate cyclases in a migratory population of embryonic neurons. Dev. Biol. 203, 15–33.

Wright, J.W., Snyder, M.A., Schwinof, K.M., Combes, S., Copenhaver, P.F., 1999. A role for fasciclin II in the guidance of neuronal migration. Development 126, 3217–3228.

Yamazaki, T., Koo, E.H., Selkoe, D.J., 1997. Cell surface amyloid beta-protein precursor colocalizes with beta 1 integrins at substrate contact sites in neural cells. J. Neurosci. 17, 1004–1010.

Yankner, B.A., 1996. Mechanisms of neuronal degeneration in Alzheimer's disease. Neuron 16, 921–932.

Zambrano, N., Bimonte, M., Arbucci, S., Gianni, D., Russo, T., Bazzicalupo, P., 2002. feh-1 and apl-1, the *Caenorhabditis* elegans orthologues of mammalian Fe65 and beta-amyloid precursor protein genes, are involved in the same pathway that controls nematode pharyngeal pumping. J. Cell Sci. 115, 1411–1422.